

EDEN Survey

Small Transiting Planet Detection Limits and Constraints on the Occurrence Rates of Planets around Late-M Dwarfs within 15 pc

Luigi Mancini

DEPARTMENT OF PHYSICS



TOR VERGATA
UNIVERSITÀ DEGLI STUDI DI ROMA



**MAX-PLANCK-INSTITUT
FÜR ASTRONOMIE**



OSSERVATORIO
ASTROFISICO DI TORINO

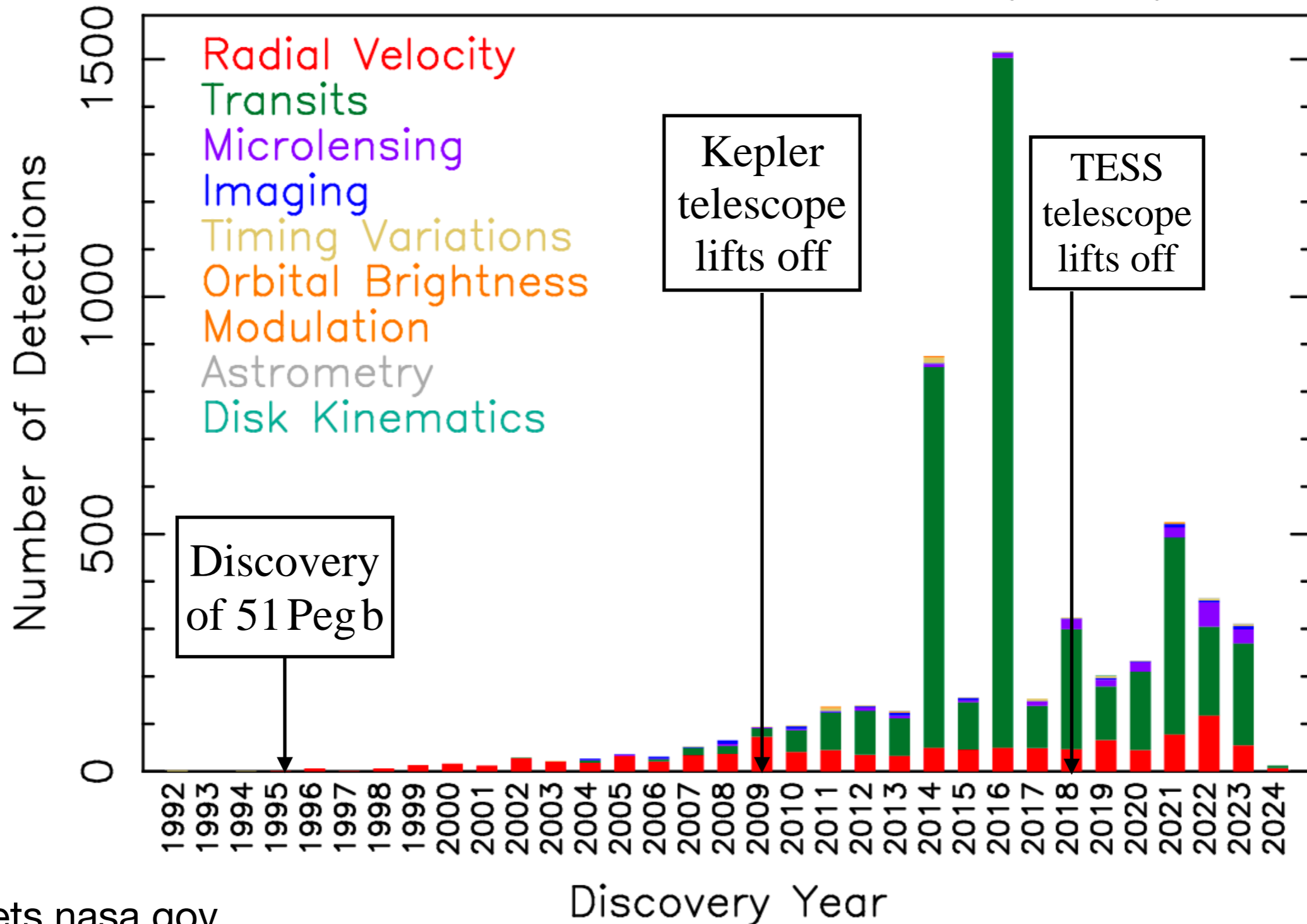
[@exoplanet LM](https://twitter.com/exoplanet_LM)



Exoplanets known today

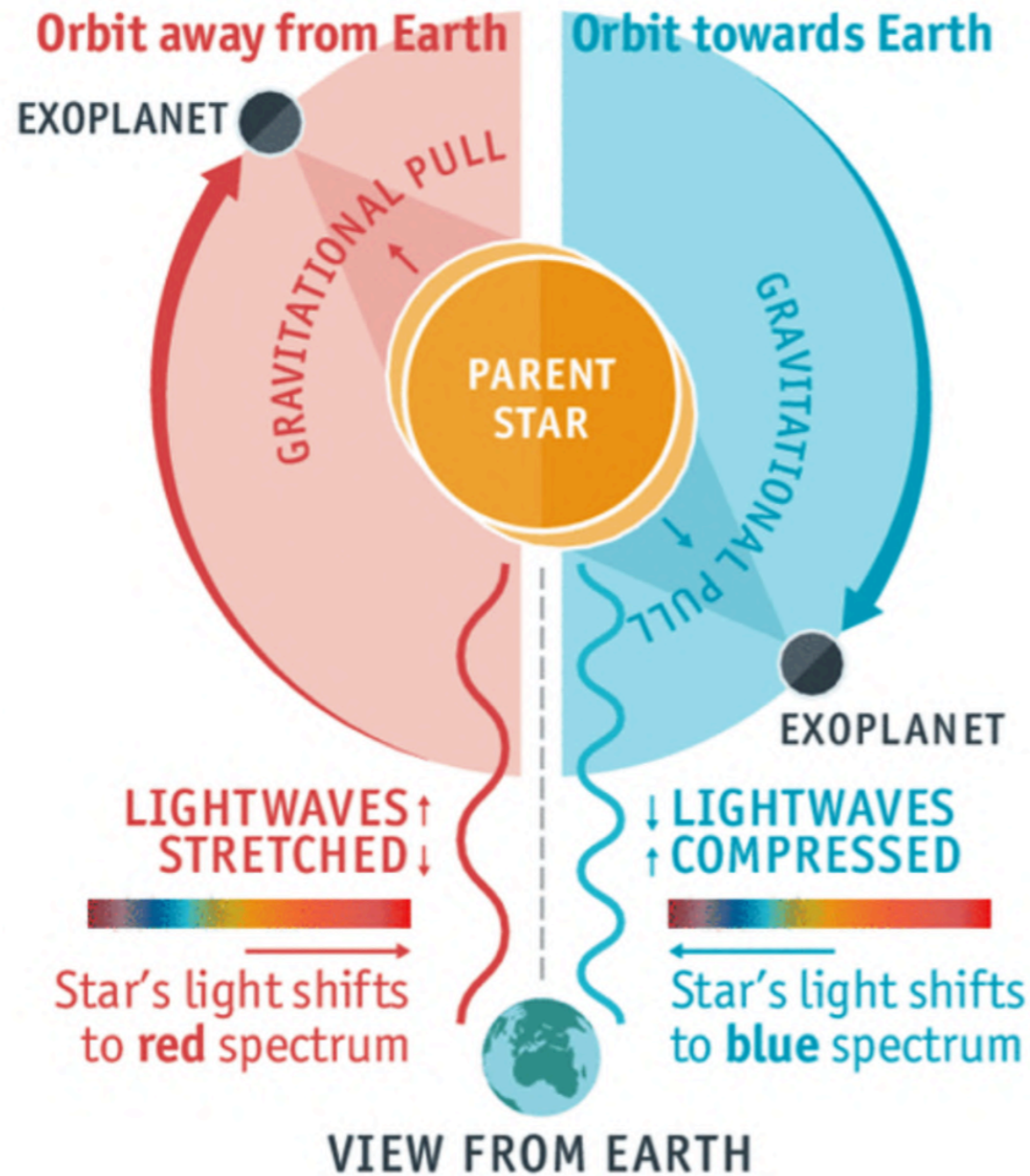
Detections Per Year

23 Feb 2024
exoplanetarchive.ipac.caltech.edu

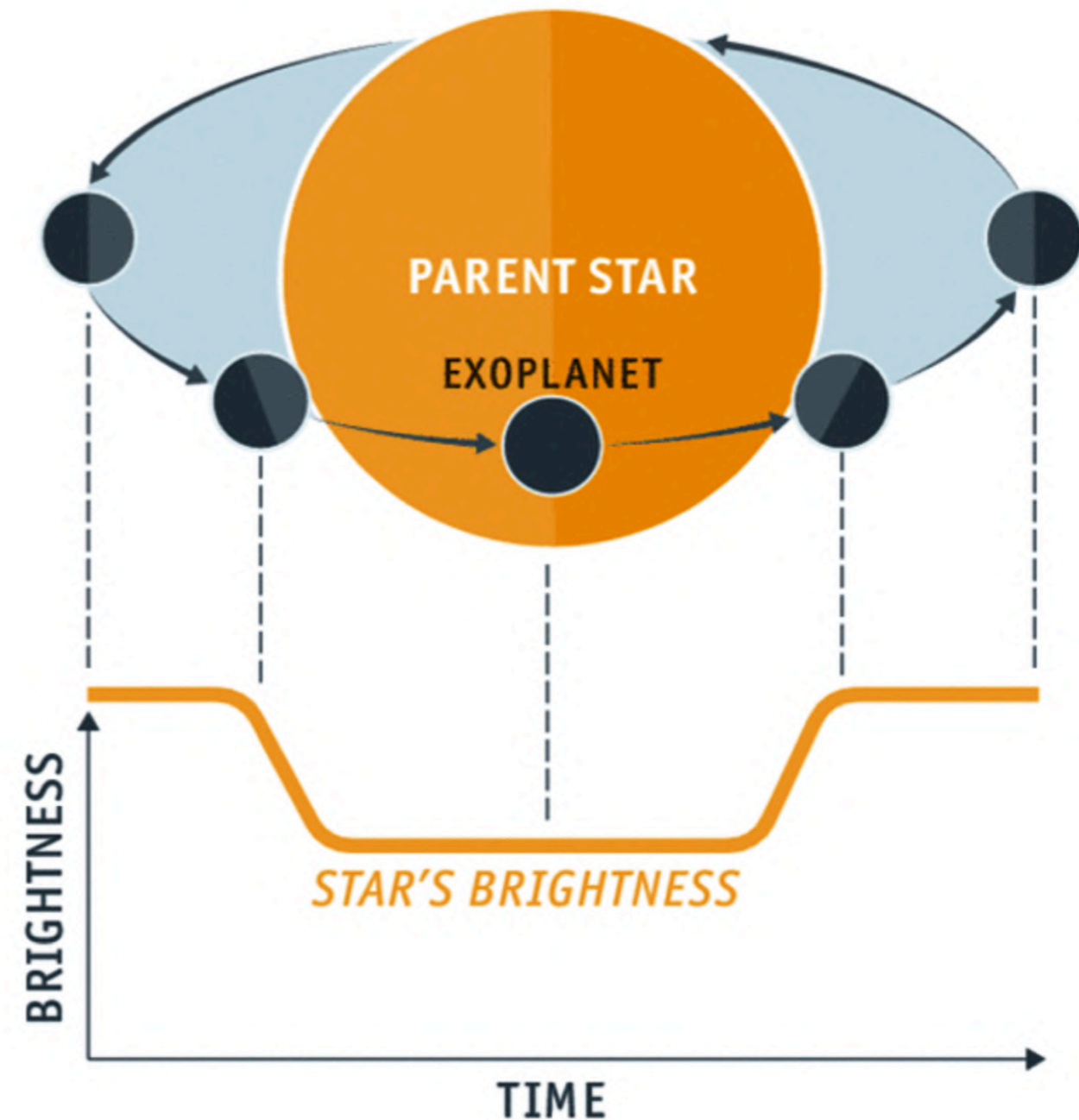


Two clever techniques to detect Exoplanets

Radial-velocity method



Transit method

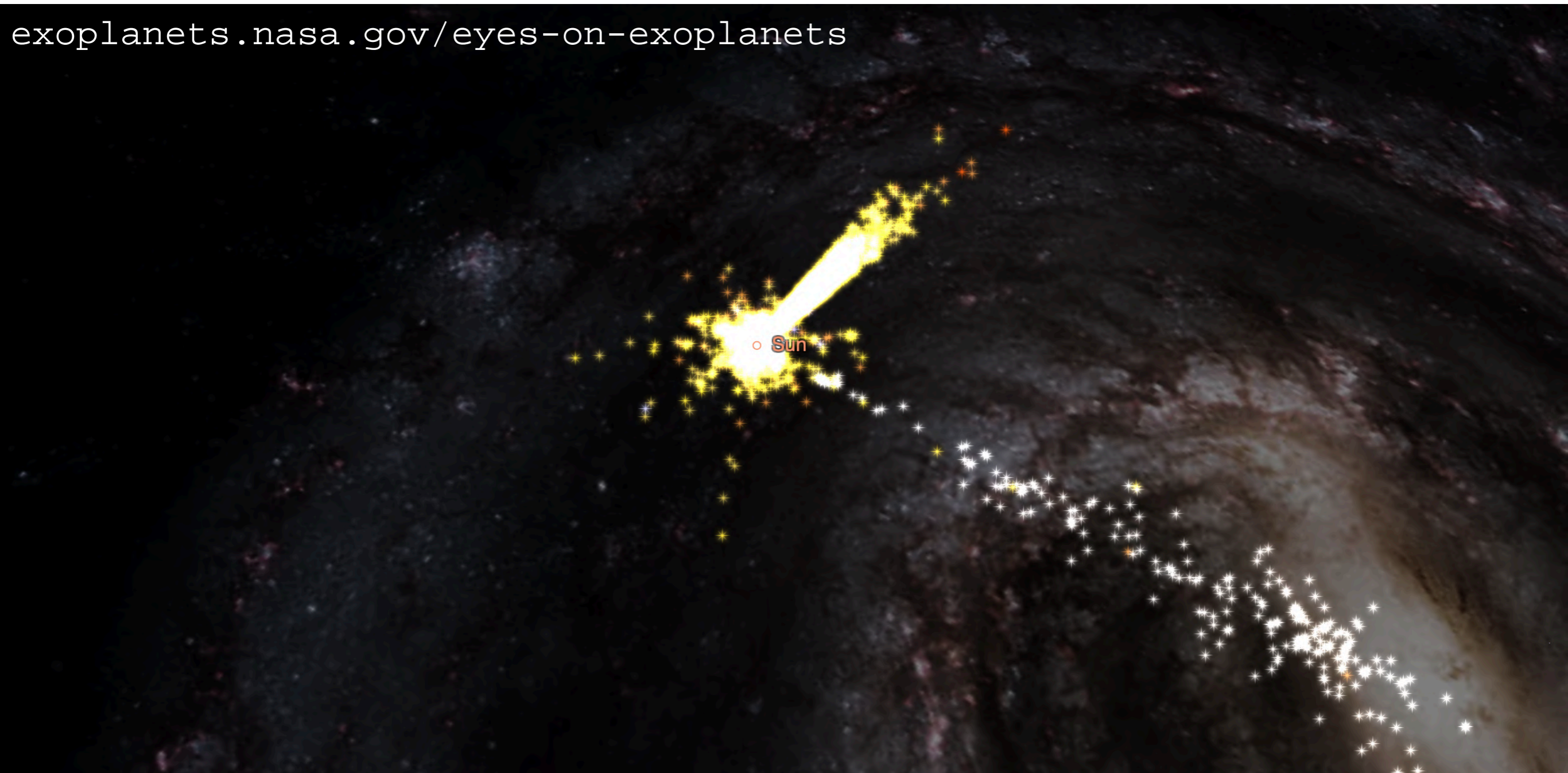


Measure the mass of the planet

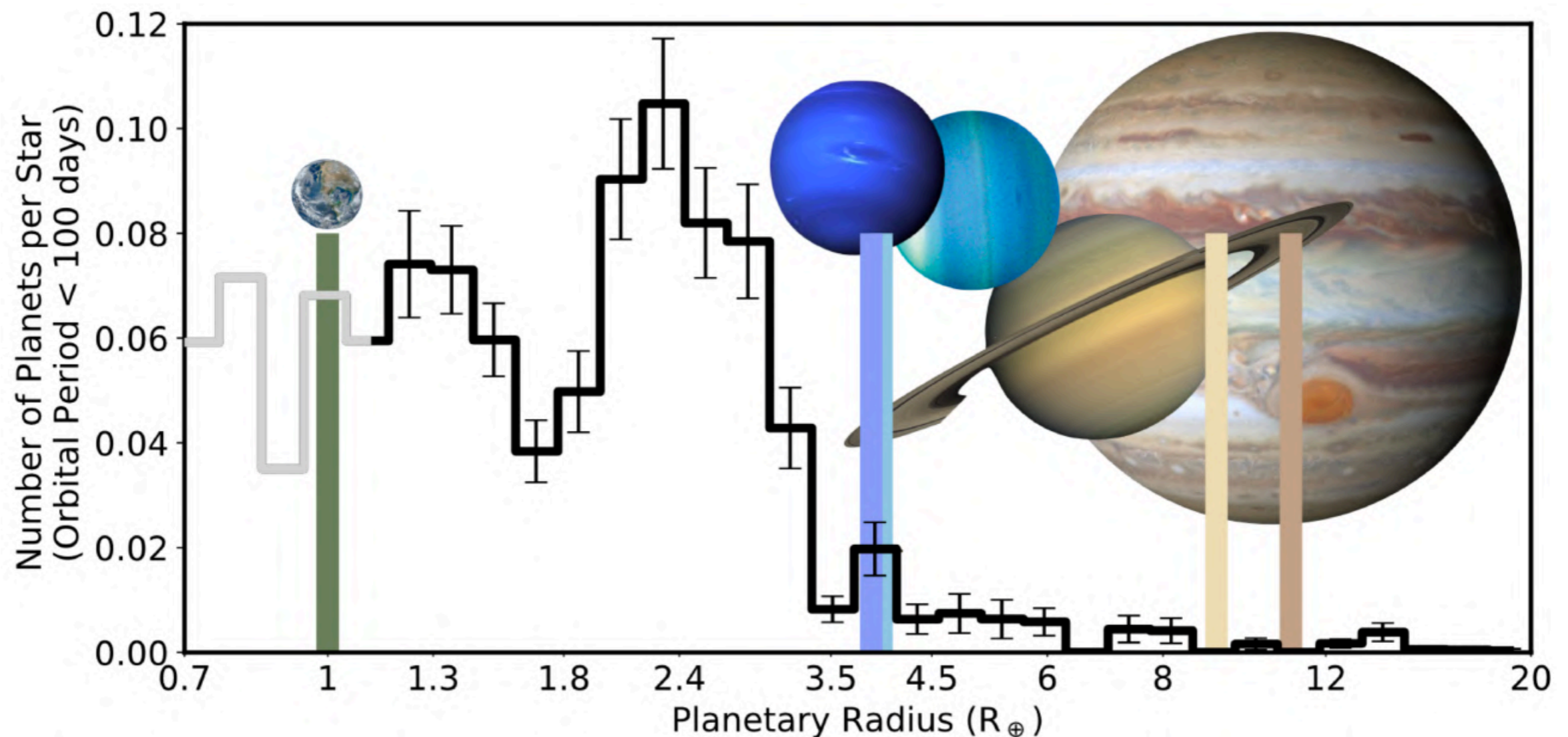
Measure the radius of the planet

- In the last decade, exoplanet research has shown that planets around other stars are incredibly common.
- Most stars are orbited by at least one planet and the most abundant types of planets are sub-Neptunes, super-Earth and rocky planets.

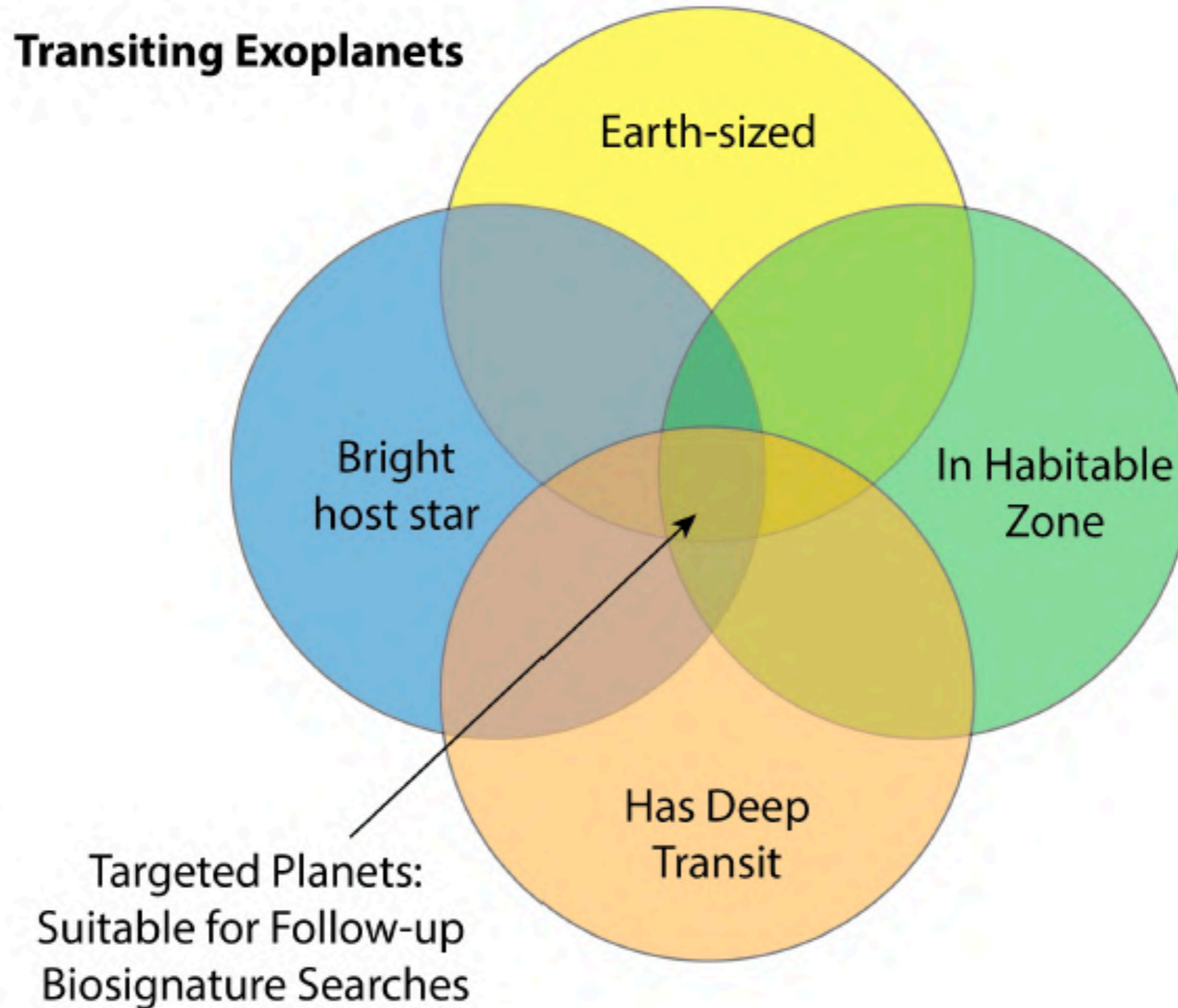
exoplanets.nasa.gov/eyes-on-exoplanets



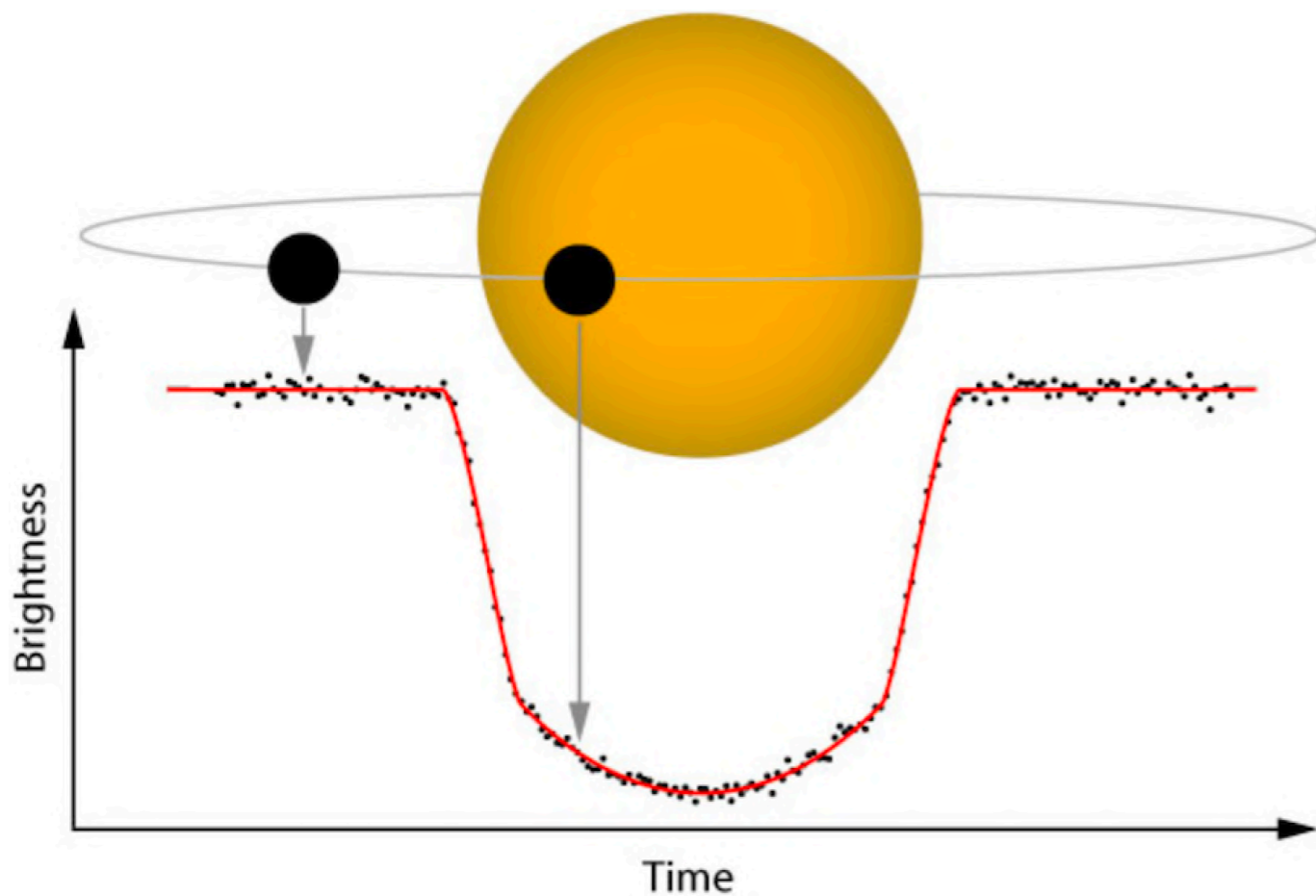
- In the legacy papers for the NASA *Kepler* Mission, it was shown that the average number of HZ planets per star, with planet radii between $0.5 R_{\oplus}$ and $1.5 R_{\oplus}$ and host star effective temperatures between 4800 and 6300 K, is $\eta_{\oplus} \approx 0.4 - 0.9$.
- With the Milky Way populated by over 300 billion stars, our galaxy alone thus hosts billions of potentially habitable planets.
- There could be from 6 to 12 terrestrial planets in the HZ around solar-type stars within just 10 pc from the Sun (e.g., Bryson et al., AJ 161, 36, 2021).



The search for planets analogous to Earth



Transits



$$\text{Transit depth} = \frac{R_p^2}{R_\star^2}$$

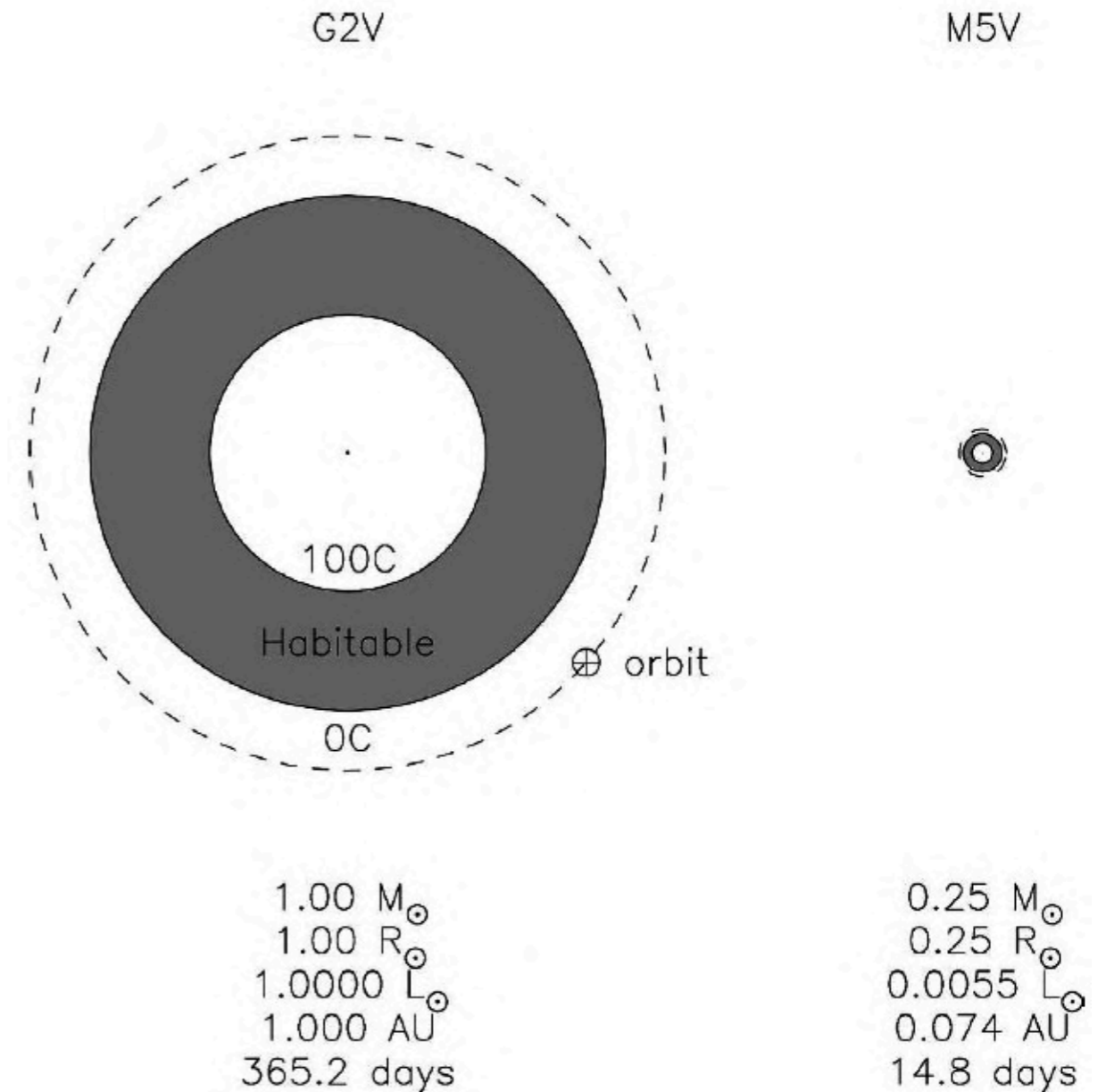
$$\text{Transit duration} = \frac{R_\star}{a}$$

Expectations for a Sun-type star

	Orbital period	Transit depth	Transit duration
Jupiter	12 years	1%	1 day
Earth	1 year	0.01%	12 hours

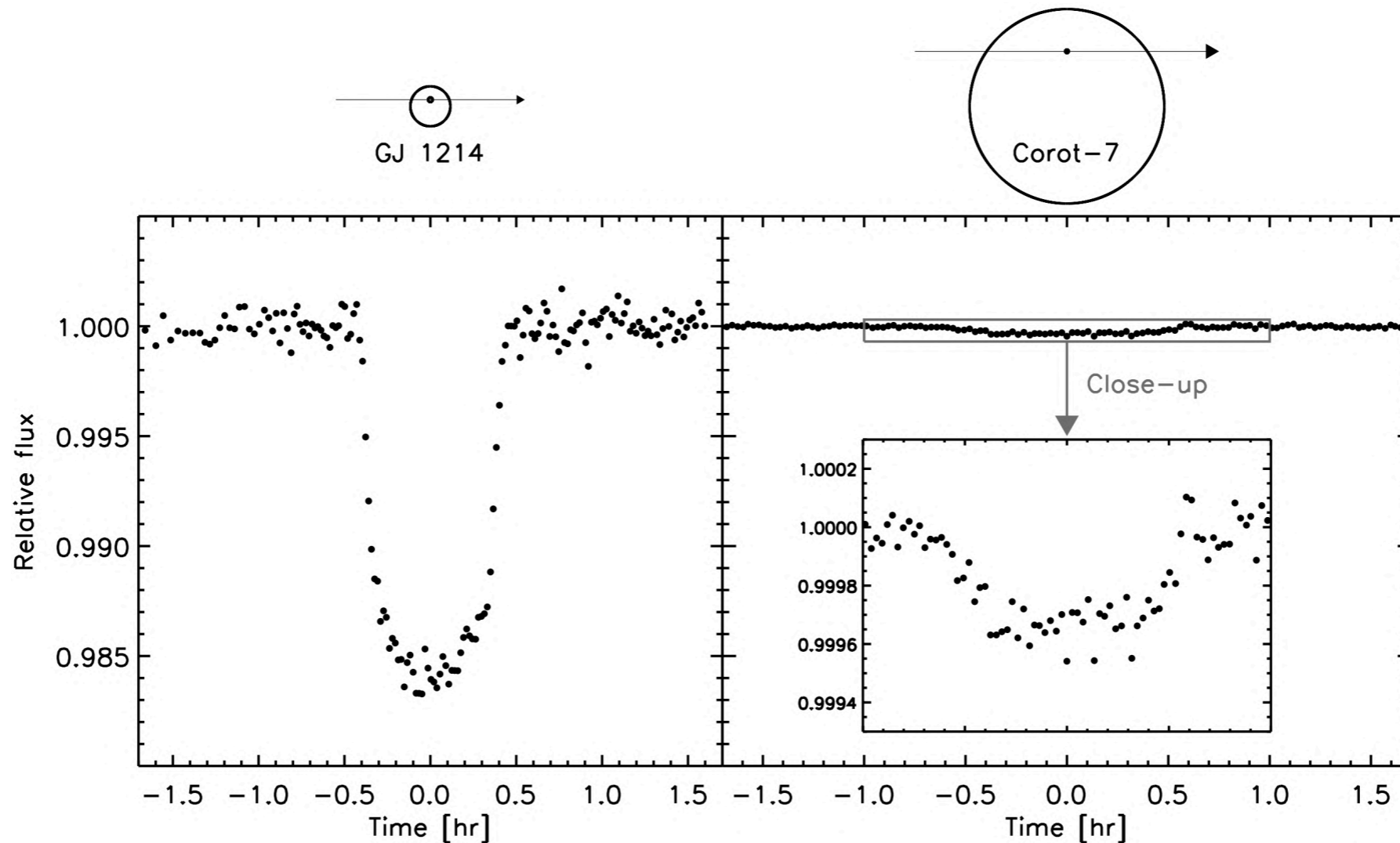
The small star opportunity

- **M dwarfs.** The specific interest of transit surveys focused on M dwarfs is that, because of their small radii, signals from a rocky planet should be readily distinguishable.
- Consider the case of a $2R_{\oplus}$ radius planet orbiting at 1 au from a G2 V star, and compare it to that of a planet of the same size orbiting an M5 V star at the distance such that it would receive the same energy per unit surface area and unit time.
Charbonneau et al., Nature 462, 891, 2009.

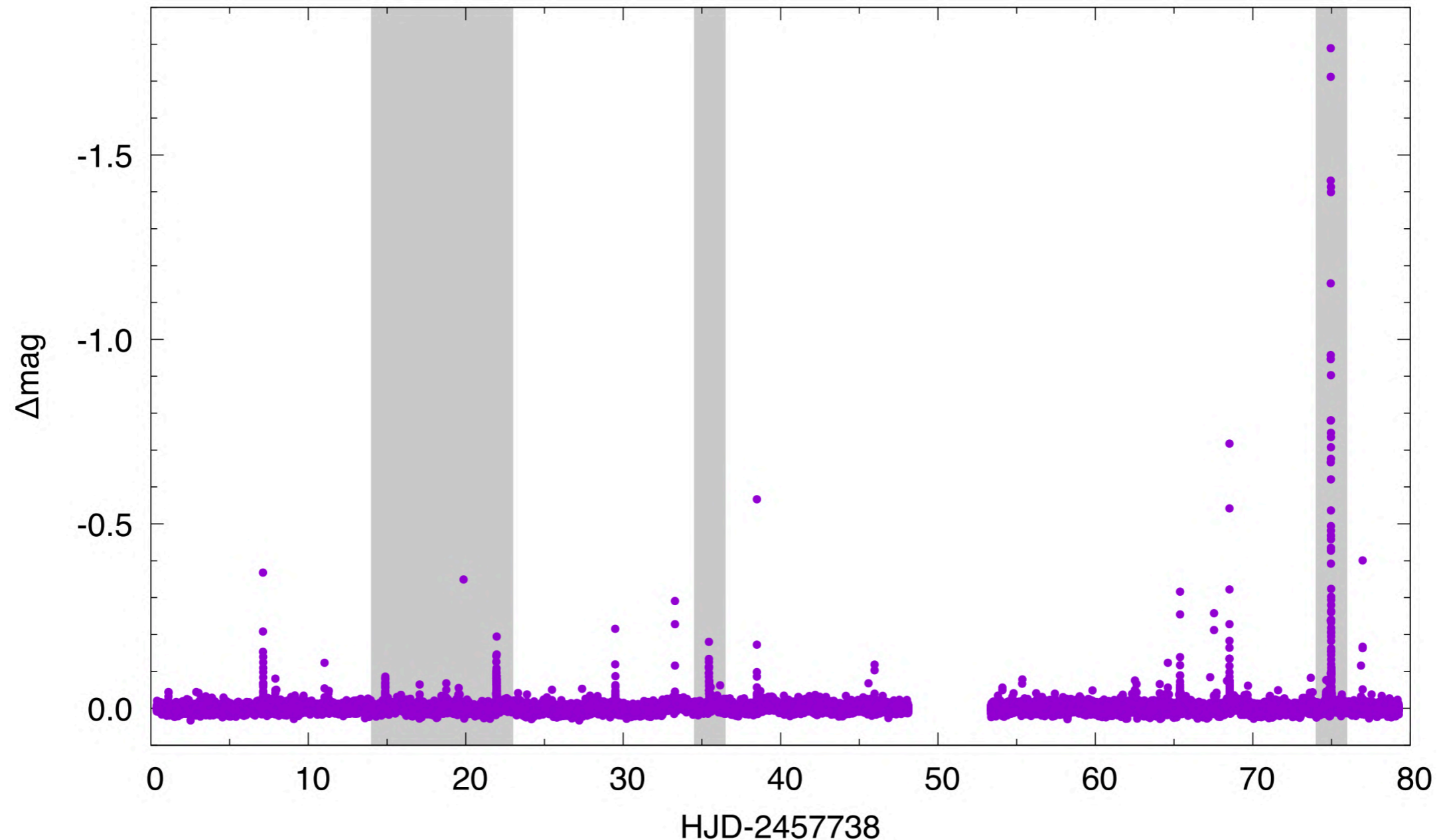


The sizes of the two orbits are drawn to scale.

- For a transit hunter, the M5 V planet presents numerous advantages:
 - transits would be more frequent: at only 0.074 au from the M5 V, the planet would orbit once every 15 days as opposed to 1 year;
 - transits would be a much larger signal: the small radius of the M5 V dwarf means that the planet would present a transit depth of 0.5% as opposed to 0.03% for a G2 V primary.

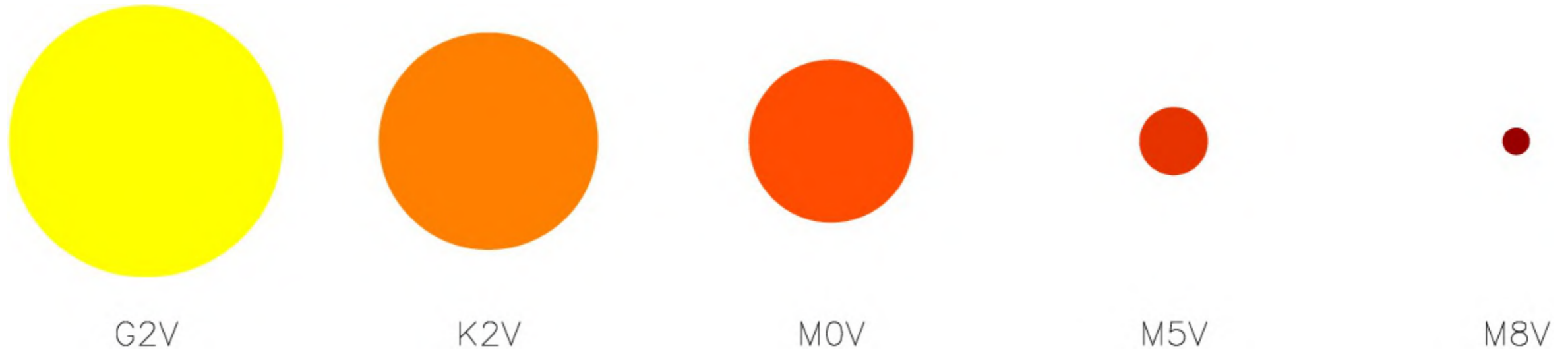


- The topic of HZ Earth-sized planets around nearby red dwarf stars has been in the spotlight over the past decade, in spite of the fact that detection of transiting planets around M-dwarfs is complicated by enhanced stellar activity, and that the habitability of some of these worlds could be influenced by stellar flares and high-energy radiation.



K2 light curve of TRAPPIST-1. Epochs where complex flare events occurred are marked with shaded areas (Vida et al., ApJ 841, 124, 2017).

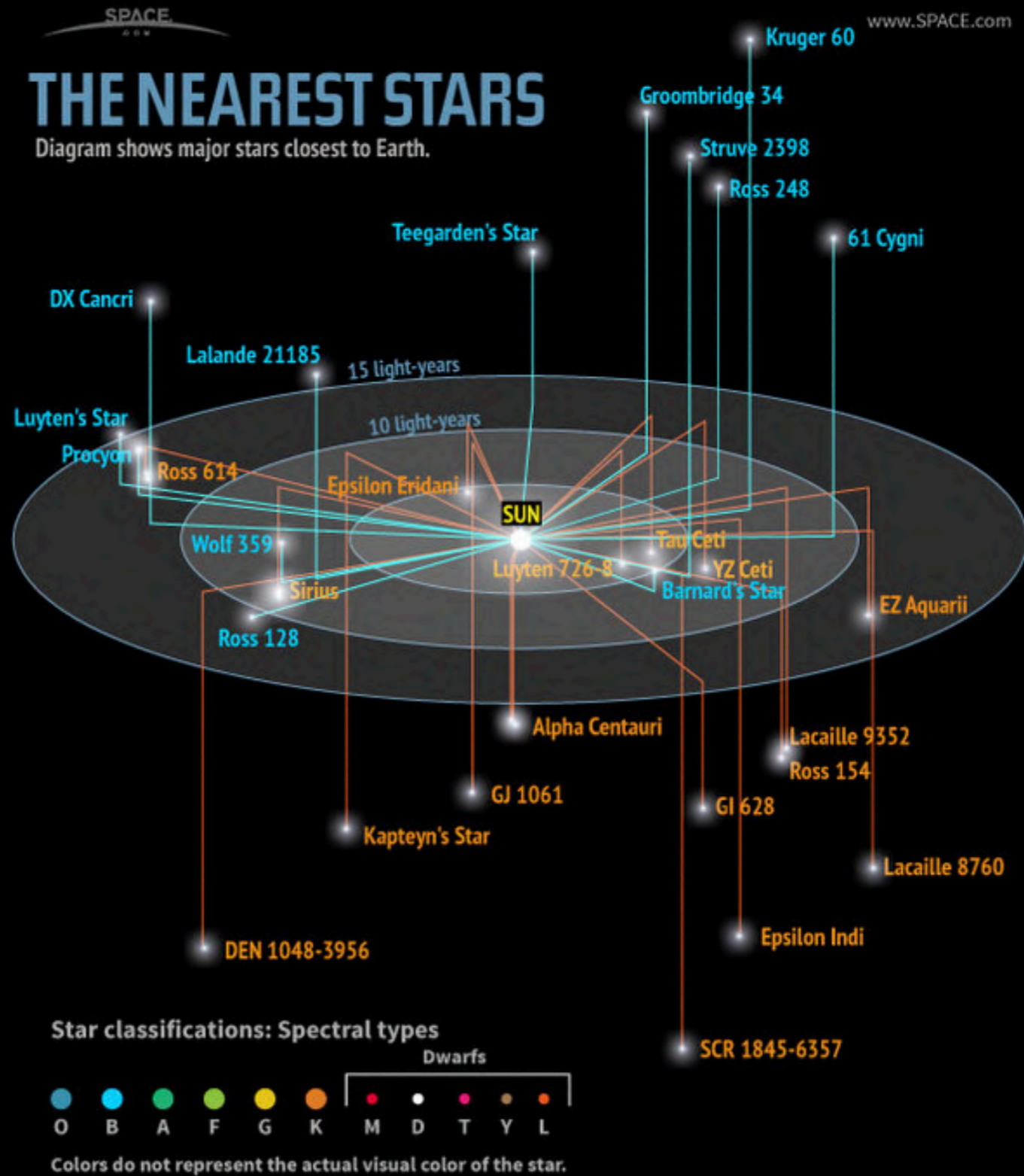
The Small Star Opportunity



Consider a super-Earth in the habitable zone:

- | | | |
|------------------------------|----------------------|-------------------------|
| ✓ Transits are deeper | <i>Sun: 0.03%</i> | <i>M-dwarf: 0.5%</i> |
| ✓ Transits are more frequent | <i>Sun: 365 days</i> | <i>M-dwarf: 15 days</i> |
| ✓ Greater Doppler Wobble | <i>Sun: 1.3 m/s</i> | <i>M-dwarf: 10 m/s</i> |

	Star system	Distance in light-years	Stellar type (s)	Observed planets
1	Alpha Centauri	4.24-4.37	M, G, K	1
2	Barnard's Star	5.96	M	1
3	Wolf 359	7.78	M	
4	Lalande 21185	8.29	M	
5	Sirius	8.58	A, D	
6	Luyten 726-8	8.73	M, M	
7	Ross 154	9.68	M	
8	Ross 248	10.32	M	
9	Epsilon Eridani	10.52	K	2
10	Lacaille 9352	10.74	M	
11	Ross 128	10.92	M	
12	EZ Aquarii	11.27	M, M, M	
13	Procyon	11.40	F, D	
14	61 Cygni	11.40	K, K	
15	Struve 2398	11.53	M, M	
16	Groombridge 34	11.62	M, M	
17	Epsilon Indi	11.82	K, T, T	
18	DX Cancri	11.83	M	
19	Tau Ceti	11.89	G	5
20	GJ 1061	11.99	M	
21	YZ Ceti	12.13	M	
22	Luyten's Star	12.37	M	
23	Teegarden's Star	12.51	M	
24	SCR 1845-6357	12.57	M, T	
25	Kapteyn's Star	12.78	M	
26	Lacaille 8760	12.87	M	
27	Kruger 60	13.15	M, M	
28	DEN 1048-3956	13.17	M	
29	UGPS 0722-05	13.26	T	
30	Ross 614	13.35	M, M	
31	WISE 1541-2250	13.70	Y	
32	WISE 0350-5658	13.70	Y	
33	Wolf 1061	13.82	M	
34	Van Maanen's Star	14.07	D	
35	Gliese 1	14.23	M	
36	Wolf 424	14.31	M, M	
37	TZ Arietis	14.51	M	
38	Gliese 687	14.80	M	
39	LHS 292	14.80	M	
40	Gliese 674	14.81	M	1
41	GJ 1245	14.81	M, M, M	
42	Gliese 440	15.06	D	
43	GJ 1002	15.31	M	
44	Gliese 876	15.34	M	4
45	LHS 288	15.61	M	
46	WISE 1405+5534	15.76	Y	
47	Gliese 412	15.83	M, M	
48	Groombridge 1618	15.85	K	
49	AD Leonis	15.94	M	
50	DENIS J081730.0-615520	16.07	T	
51	Gliese 832	16.08	M	1
52	LP 944-020	16.19	M	
53	DEN 0255-4700	16.20	L	





THE MEARTH PROJECT

WELCOME SCIENCE TEAM TELESCOPES DISCOVERIES DATA

<https://lweb.cfa.harvard.edu/MEarth/>



- MEarth-North started operations in 2008, while MEarth-South in 2014.
- Two stations for a total of $16 \times 0.4\text{m}$ telescopes.
- 3 detections.
 - GJ1214 b Charbonneau et al., Nature 462, 891 (2009)
 - GJ1132 b Berta-Thompson et al., Nature 527, 204 (2015)
 - LHS1140b Dittmann et al., Nature 544, 333 (2017)

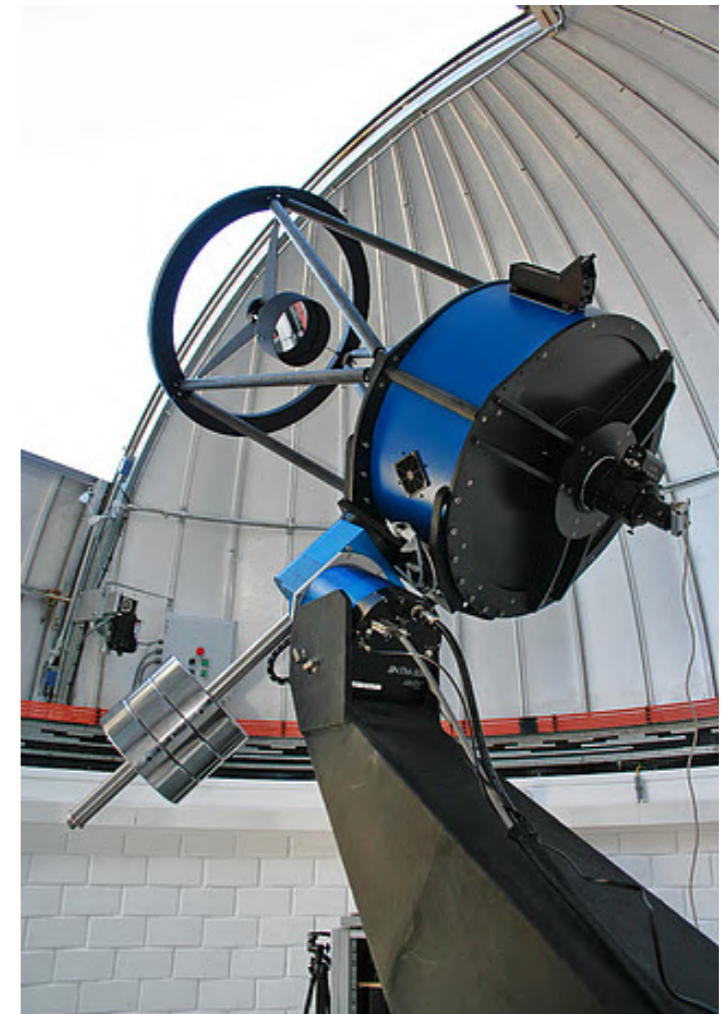
THE APACHE PROJECT

<http://apacheproject.altervista.org/>

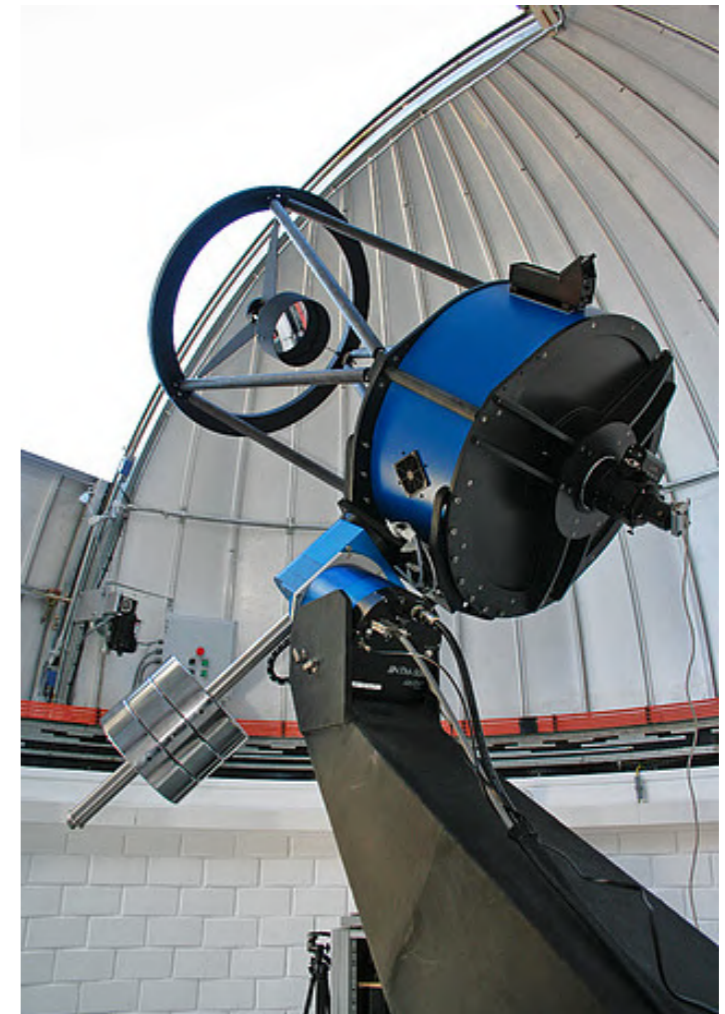
- The APACHE station was located in at the Observatory of Valle d'Aosta (Saint-Barthélemy).
 - $5 \times 0.4\text{m}$ telescopes.
 - APACHE worked from 2011 to 2018.
 - 0 detections
-
- Giacobbe et al. 2012, MNRAS, 424, 3101
 - Giacobbe et al. 2020, MNRAS, 491, 5216



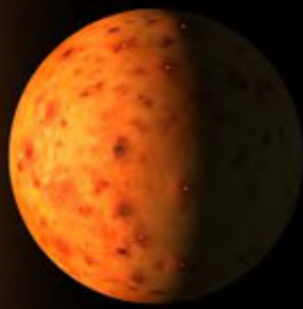
- **TRAPPIST.** The Belgian Transiting Planets and Planetesimals Small Telescope (TRAPPIST) originally comprised a 0.6-m robotic telescope at La Silla, Chile, operational since 2010.
- It aims to identify transiting exoplanets and comets, as well as monitoring WASP systems (Gillon et al., 2012b; Delrez et al., 2014; Hellier et al., 2014).
- The TRAPPIST UCD (Ultra Cool Dwarf) transit survey has observed 50 brightest southern UCDs for about 100 hr (Gillon et al. 2011; Jehin et al. 2011).



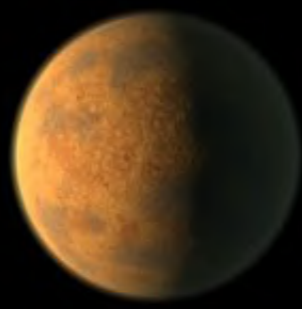
- The first and only discovery, TRAPPIST-1 ($V = 18.8$ mag), was originally discovered as a 3-planet transiting system around an ultracool dwarf at a distance of 12 pc (Gillon et al., 2016), and later recognised as a 7-planet transiting system, with the planets all of terrestrial mass probably orbiting within their habitable zone (Gillon et al., 2017).



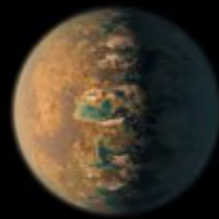
TRAPPIST-1 System



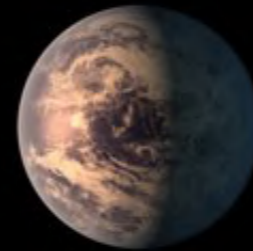
b



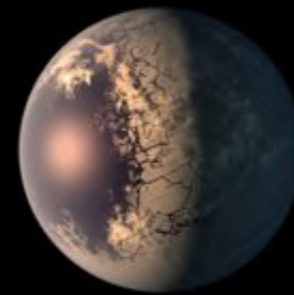
c



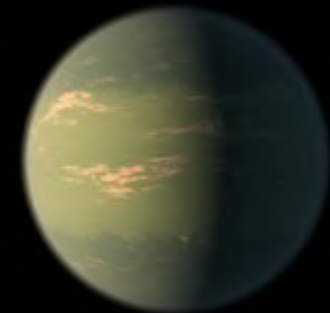
d



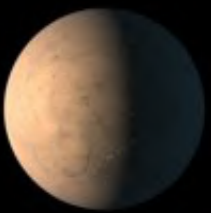
e



f



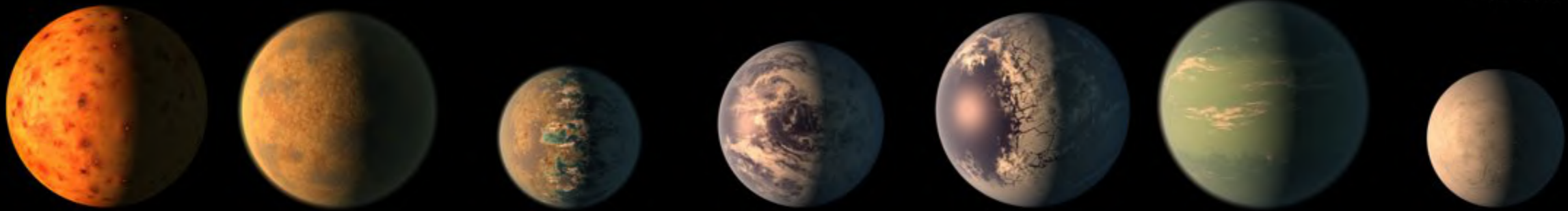
g



h

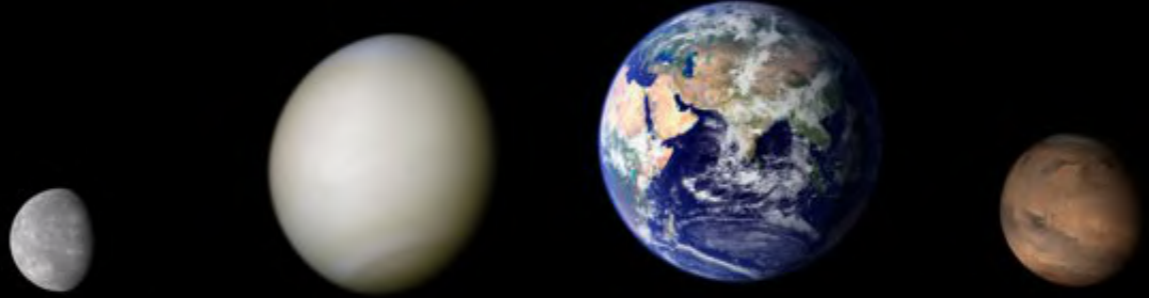
Illustration

TRAPPIST-1 System

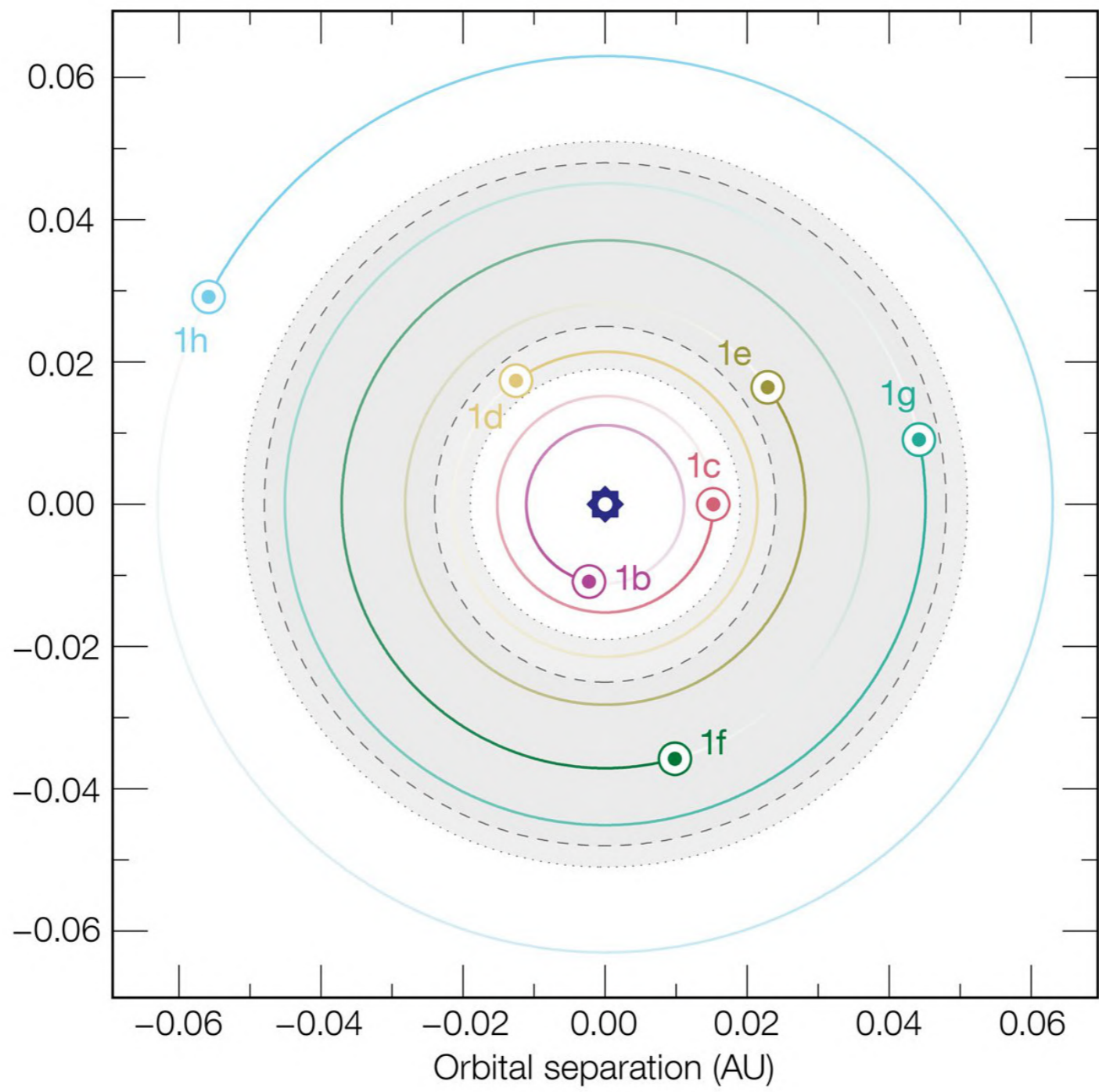


	b	c	d	e	f	g	h
Orbital Period <i>days</i>	1.51 days	2.42 days	4.05 days	6.10 days	9.21 days	12.35 days	~20 days
Distance to Star <i>Astronomical Units (AU)</i>	0.011 AU	0.015 AU	0.021 AU	0.028 AU	0.037 AU	0.045 AU	~0.06 AU
Planet Radius <i>relative to Earth</i>	1.09 R_{earth}	1.06 R_{earth}	0.77 R_{earth}	0.92 R_{earth}	1.04 R_{earth}	1.13 R_{earth}	0.76 R_{earth}
Planet Mass <i>relative to Earth</i>	0.85 M_{earth}	1.38 M_{earth}	0.41 M_{earth}	0.62 M_{earth}	0.68 M_{earth}	1.34 M_{earth}	—

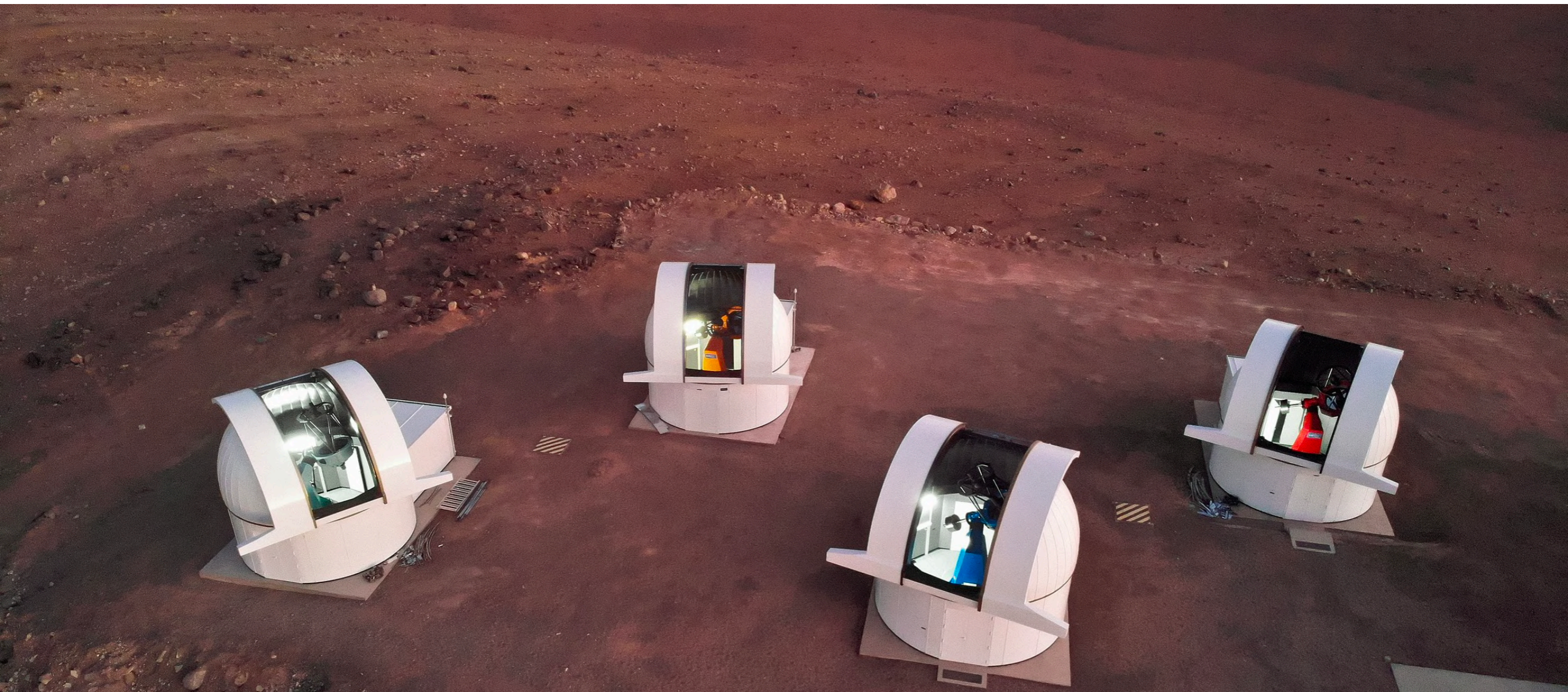
Solar System
Rocky Planets




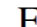




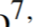
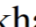

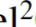

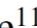
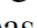
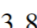
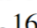


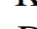
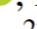
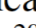
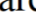
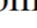
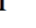
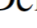
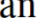
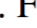
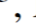
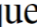
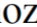
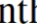
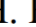

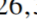

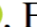

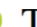
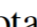
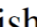
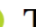

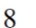

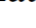




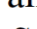
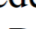
	Mercury	Venus	Earth	Mars
Orbital Period <i>days</i>	87.97 days	224.70 days	365.26 days	686.98 days
Distance to Star <i>Astronomical Units (AU)</i>	0.387 AU	0.723 AU	1.000 AU	1.524 AU
Planet Radius <i>relative to Earth</i>	0.38 R_{earth}	0.95 R_{earth}	1.00 R_{earth}	0.53 R_{earth}
Planet Mass <i>relative to Earth</i>	0.06 M_{earth}	0.82 M_{earth}	1.00 M_{earth}	0.11 M_{earth}



- The TRAPPIST UCD transit survey served as a prototype for a more ambitious search for exoplanets around UCDs, i.e. SPECULOOS.
- SPECULOOS stands for Search for habitable Planets EClipsing ULtra-cOOl Stars and it is a ground-based transit survey led by the University of Liège (Belgium), which consists of six identical 1-m robotic telescopes.
- 4 telescopes are located at Paranal, 2 at Teide Observatory, and are optimised for detecting Earth-size planets transiting the nearest ultra-cool dwarfs.



Two temperate super-Earths transiting a nearby late-type M dwarf★

L. Delrez^{1,2} [✉], C. A. Murray^{3,4} [✉], F. J. Pozuelos^{1,2,5} [✉], N. Narita^{6,7,8} [✉], E. Ducrot⁹ [✉], M. Timmermans¹, N. Watanabe¹⁰ [✉], A. J. Burgasser¹¹ [✉], T. Hirano^{7,12} [✉], B. V. Rackham^{13,14} [✉], K. G. Stassun¹⁵ [✉], V. Van Grootel² [✉], C. Aganze¹¹ [✉], M. Cointepas^{16,17}, S. Howell¹⁸ [✉], L. Kaltenegger¹⁹ [✉], P. Niraula¹³ [✉], D. Sebastian²⁰ [✉], J. M. Almenara¹⁶, K. Barkaoui^{1,13,8} [✉], T. A. Baycroft²⁰, X. Bonfils¹⁶ [✉], F. Bouchy¹⁷ [✉], A. Burdanov¹³ [✉], D. A. Caldwell^{18,21}, D. Charbonneau²² [✉], D. R. Ciardi²³ [✉], K. A. Collins²², T. Daylan^{14,24,25} [✉], B.-O. Demory²⁶ [✉], J. de Wit¹³, G. Dransfield²⁰ [✉], S. B. Fajardo-Acosta²³, M. Fausnaugh¹⁴ [✉], A. Fukui^{6,8} [✉], E. Furlan²³ [✉], L. J. Garcia¹ [✉], C. L. Gnilka¹⁸, Y. Gómez Maqueo Chew²⁷ [✉], M. A. Gómez-Muñoz²⁸ [✉], M. N. Günther²⁹ [✉], H. Harakawa³⁰, K. Heng^{26,31} [✉], M. J. Hooton³ [✉], Y. Hori^{7,12} [✉], M. Ikoma¹² [✉], E. Jehin² [✉], J. M. Jenkins¹⁸ [✉], T. Kagetani¹⁰ [✉], K. Kawauchi^{8,32} [✉], T. Kimura³³, T. Kodama⁶ [✉], T. Kotani^{7,12,34}, V. Krishnamurthy^{7,12} [✉], T. Kudo³⁰ [✉], V. Kunovac^{35,20} [✉], N. Kusakabe^{7,12} [✉], D. W. Latham²² [✉], C. Littlefield^{36,18}, J. McCormac³¹, C. Melis¹¹ [✉], M. Mori³⁷ [✉], F. Murgas^{8,32} [✉], E. Pallé^{8,32} [✉], P. P. Pedersen³, D. Queloz³ [✉], G. Ricker^{14,24} [✉], L. Sabin²⁸ [✉], N. Schanche²⁶, U. Schroffenegger²⁶, S. Seager^{13,14,24,38}, B. Shiao³⁹, S. Sohy², M. R. Standing²⁰ [✉], M. Tamura^{37,7,12} [✉], C. A. Theissen¹¹ [✉], S. J. Thompson³ [✉], A. H. M. J. Triaud²⁰ [✉], R. Vanderspek¹⁴ [✉], S. Vievard^{7,30} [✉], R. D. Wells²⁶ [✉], J. N. Winn²⁵, Y. Zou¹⁰ [✉], S. Zúñiga-Fernández¹ [✉], and M. Gillon¹ [✉]

Context. In the age of JWST, temperate terrestrial exoplanets transiting nearby late-type M dwarfs provide unique opportunities for characterising their atmospheres, as well as searching for biosignature gases. In this context, the benchmark TRAPPIST-1 planetary system has garnered the interest of a broad scientific community.

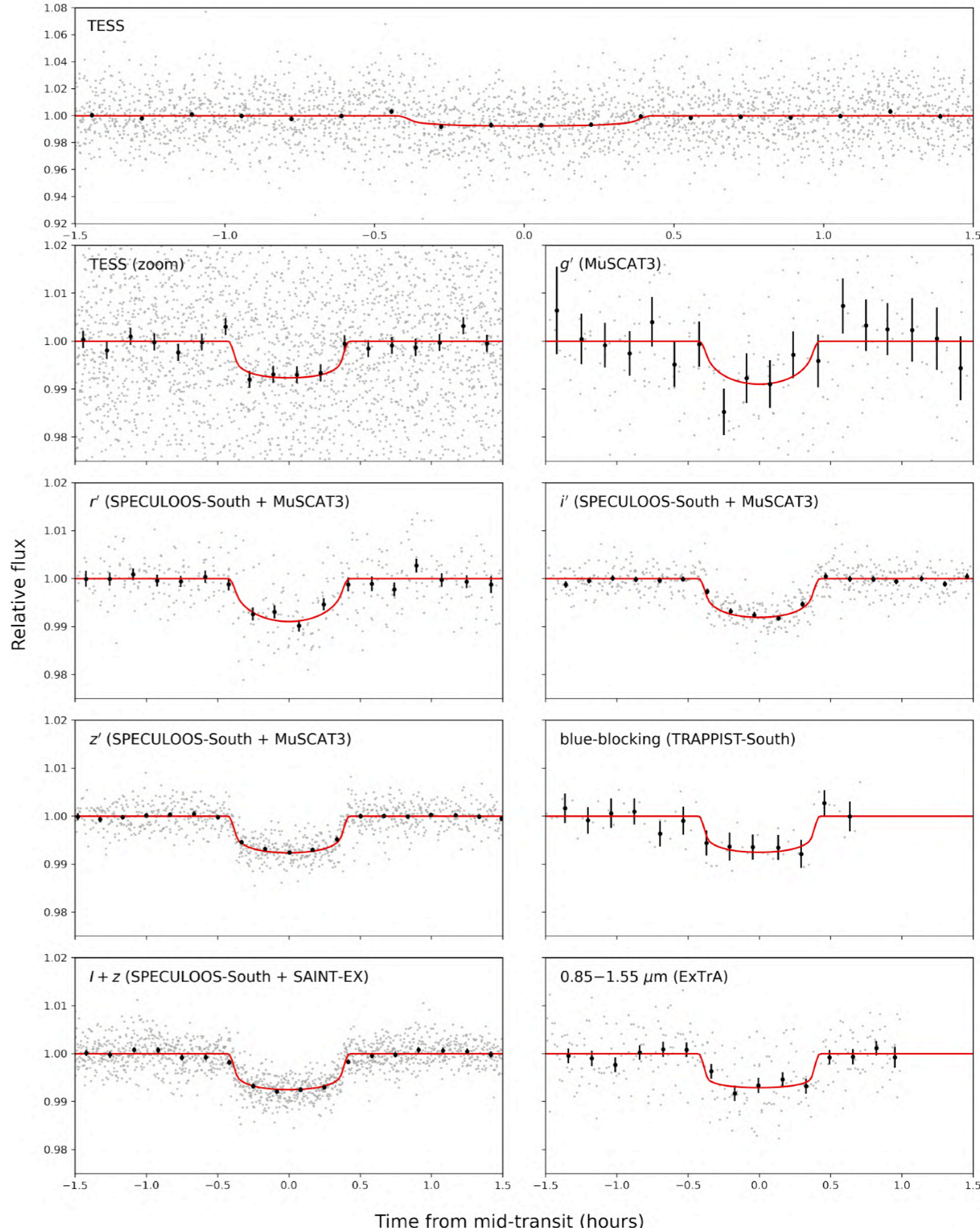
Aims. We report here the discovery and validation of two temperate super-Earths transiting LP 890-9 (TOI-4306, SPECULOOS-2), a relatively low-activity nearby (32 pc) M6V star. The inner planet, LP 890-9 b, was first detected by TESS (and identified as TOI-4306.01) based on four sectors of data. Intensive photometric monitoring of the system with the SPECULOOS Southern Observatory then led to the discovery of a second outer transiting planet, LP 890-9 c (also identified as SPECULOOS-2 c), previously undetected by TESS. The orbital period of this second planet was later confirmed by MuSCAT3 follow-up observations.

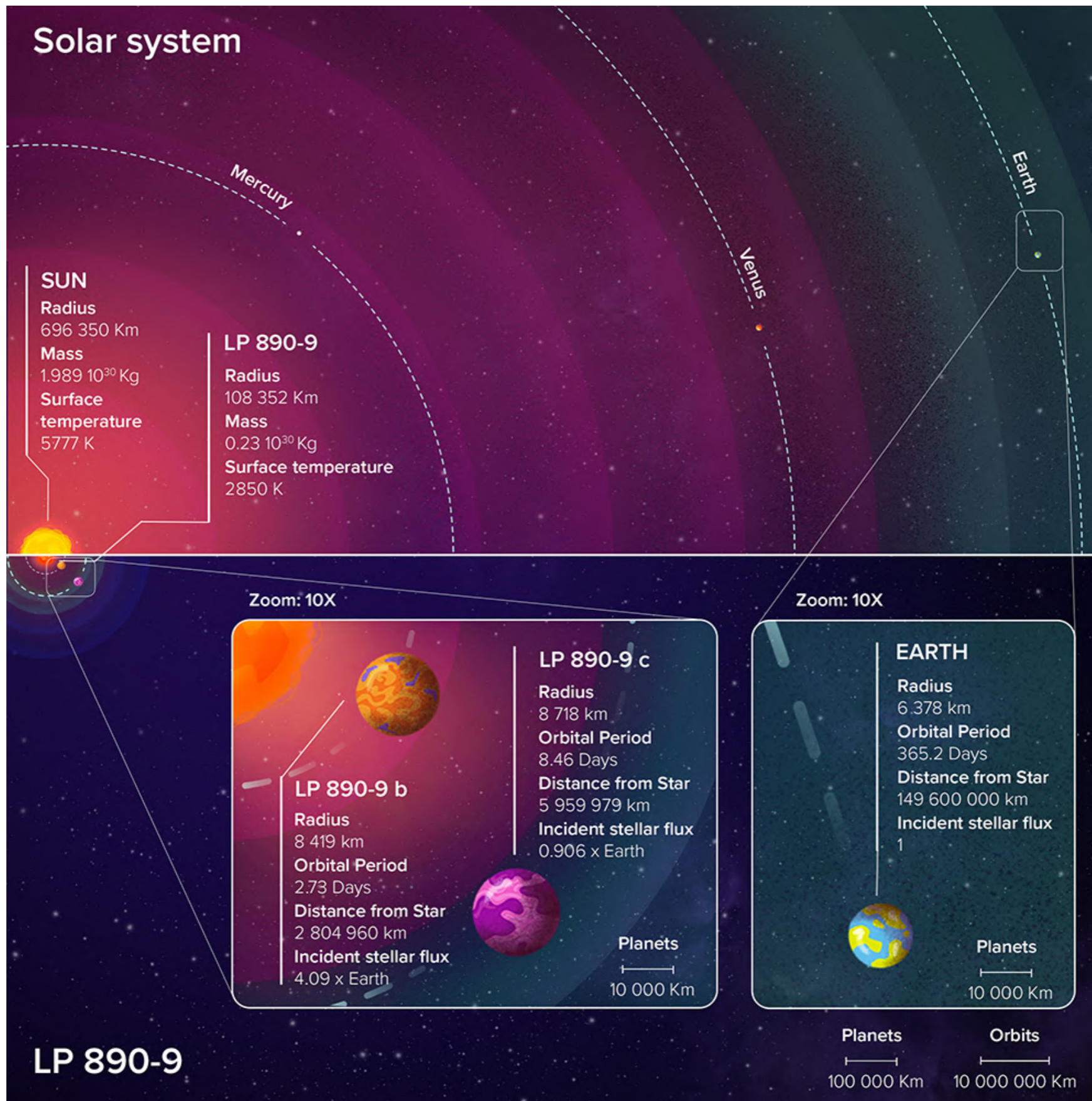
Methods. We first inferred the properties of the host star by analyzing its Lick/Kast optical and IRTF/SpeX near-infrared spectra, as well as its broadband spectral energy distribution, and *Gaia* parallax. We then derived the properties of the two planets by modelling multi-colour transit photometry from TESS, SPECULOOS-South, MuSCAT3, ExTrA, TRAPPIST-South, and SAINT-EX. Archival imaging, Gemini-South/Zorro high-resolution imaging, and Subaru/IRD radial velocities also support our planetary interpretation.

Results. With a mass of $0.118 \pm 0.002 M_{\odot}$, a radius of $0.1556 \pm 0.0086 R_{\odot}$, and an effective temperature of 2850 ± 75 K, LP 890-9 is the second-coolest star found to host planets, after TRAPPIST-1. The inner planet has an orbital period of 2.73 d, a radius of $1.320^{+0.053}_{-0.027} R_{\oplus}$, and receives an incident stellar flux of $4.09 \pm 0.12 S_{\oplus}$. The outer planet has a similar size of $1.367^{+0.055}_{-0.039} R_{\oplus}$ and an orbital period of 8.46 d. With an incident stellar flux of $0.906 \pm 0.026 S_{\oplus}$, it is located within the conservative habitable zone, very close to

Photometric magnitudes

TESS (mag)	14.2683 ± 0.0076
V (mag)	18.0 ± 0.2
<i>g</i> (mag)	18.4422 ± 0.0072
<i>r</i> (mag)	17.1365 ± 0.0050
<i>i</i> (mag)	15.0975 ± 0.0026
<i>z</i> (mag)	14.1593 ± 0.0013
<i>y</i> (mag)	13.6454 ± 0.0044
<i>Gaia</i> (mag)	15.7913 ± 0.0028
<i>J</i> (mag)	12.258 ± 0.023
<i>H</i> (mag)	11.692 ± 0.025
<i>K</i> (mag)	11.344 ± 0.023
Distance (pc)	32.33 ± 0.05

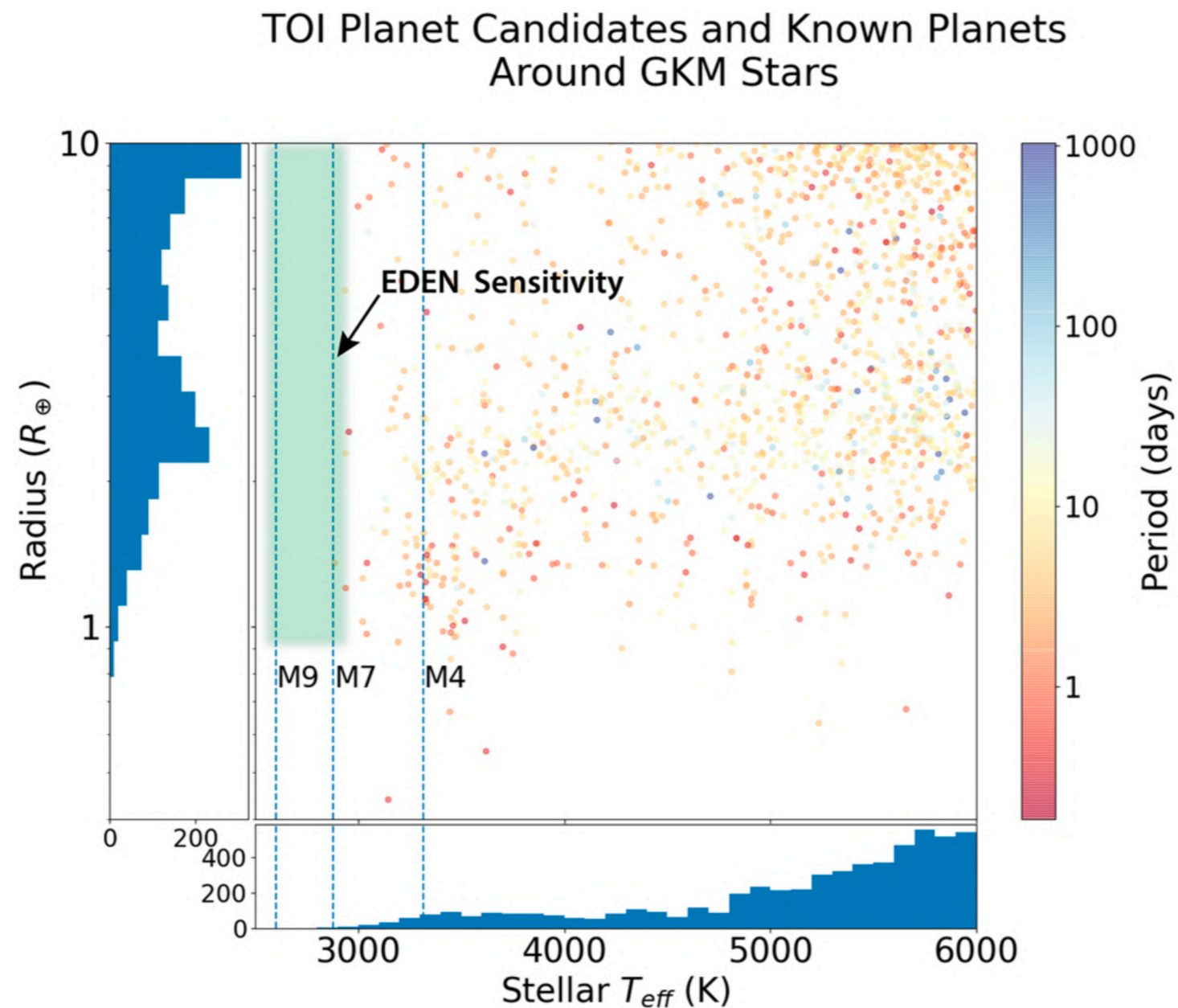




Delrez et al., A&A 667, A59 (2022)

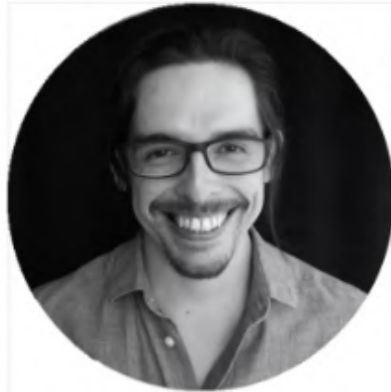
- Most current surveys studying planets around M dwarfs have some level of biases.
 - Only ~1% of the 186,000 stars in the *Kepler* sample are M dwarfs (Berger et al. 2020).
 - Only ~17% of the 220,000 stars in the *K2* sample are M dwarfs (Hardegree-Ullman et al. 2020).
- Only a small set of planets around mid-M dwarfs was detected from *Kepler* data.
- Stars with masses between 0.1 and 0.5 M_{\odot} , the M dwarfs, are not as thoroughly explored, especially near the low end of the mass range. The occurrence rate planets around M dwarfs is poorly understood.
- The occurrence rate of short-period (0.5–10 days) small planets ($0.5 - 2.5 R_{\oplus}$) is higher for mid-M dwarfs than for early-M dwarfs (Hardegree-Ullman et al. 2019)
 - mid-M dwarfs: ~1.19 planets per star
 - early-M dwarfs: ~0.63 planets per star
- This trend continues to the lowest-mass stars, consistent with the lower limit on planet occurrence around late-M dwarfs implied by the detection of TRAPPIST-1 (Lienhard et al. 2020).

- RV surveys like CARMENES and HADES (Sabotta et al. 2021; Pinamonti et al. 2022; I. Ribas et al. 2023) are not sensitive to later M dwarfs with current technological limits.
- Also TESS is not sensitive to later M.
- Targeted surveys to detect exoplanets around mid- to late-M dwarfs are necessary to understand planet occurrence near the substellar boundary better.





- The EDEN team searched for habitable worlds within 50 ly from the northern hemisphere.
- The survey was focussed on mid- to late-M type stars for habitable-zone Earth-sized planets.
- A network of seven professional medium-sized (1m-class) telescopes was used to perform the deepest photometric monitoring campaign of 22 nearby late-M dwarf stars, using data from over 500 nights collected between 2018 and 2023 (5 yr).
- Gibbs et al. 2020, AJ 159, 169;
- Dietrich et al. 2023, AJ 165, 149.



Nestor Espinoza
EDEN Expert

Bernoulli Postdoctoral Fellow at Max Planck Institute for Astronomy, Heidelberg. EDEN Photometry and Transit Forecast Teams.



Martin Schlecker
EDEN Graduate Student

Astronomy Graduate Student at the Max Planck Institute for Astronomy, Heidelberg. EDEN Observing Team and EDEN Targets Team



Marton Apai
EDEN Expert

Chief Technology Officer, IT Project Manager, Senior Software Engineer EDEN Software Development Expert



Luigi Mancini
EDEN Science Team

Senior Research Staff Scientist at the University of Rome Tor Vergata



Thomas K. Henning
EDEN Steering Committee

Director of the Planet and Star Formation Group at the Max Planck Institute for Astronomy, Heidelberg



Jose Perez Chavez
EDEN Undergraduate Student, Data Reduction Team

UA Astronomy/Astrobiology Undergraduate Student



Kerst Kingsbury
UA Undergraduate Student, EDEN Observations Team

University of Arizona Mining Engineering and Planetary Science undergraduate student



Allie Mousseau
EDEN Astronomy Student

Astronomy student at The University of Arizona, and member of the EDEN Targets Team



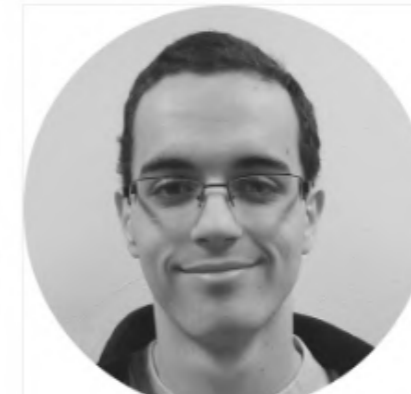
Daniel Apai
EDEN Founder

Associate Professor of Astronomy and Planetary Sciences at The University of Arizona. Apai's blog (apai.space) covers news and thoughts related to exoplanet exploration and astrobiology.



Benjamin Rackham
EDEN Graduate Student

Astronomy graduate student at the Steward Observatory of The University of Arizona.



Alex Bixel
EDEN Graduate Student

Astronomy graduate student and NASA Earth and Space Science Fellow at the Steward Observatory of the University of Arizona.



Paul Gabor
Steering Committee member

Astronomer and Vice Directory of the Vatican Observatory Research Group.

EDEN Team

Steward Observatory, University of Arizona
Max Planck Institute for Astronomy, Heidelberg
University of Tor Vergata, Rome
NCU Taiwan

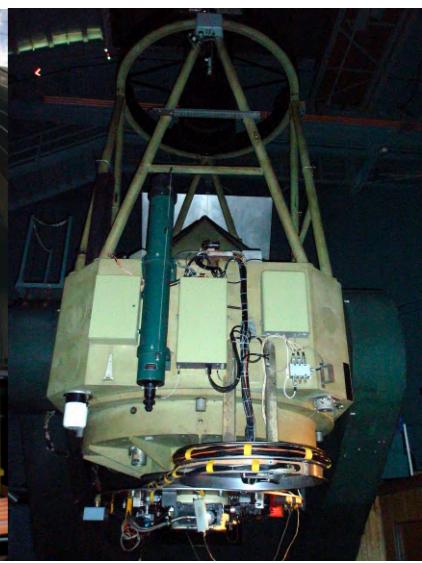
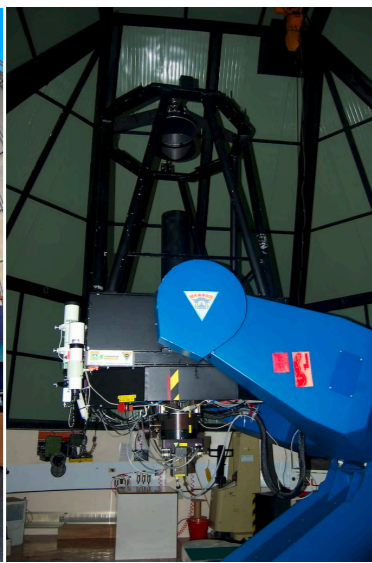
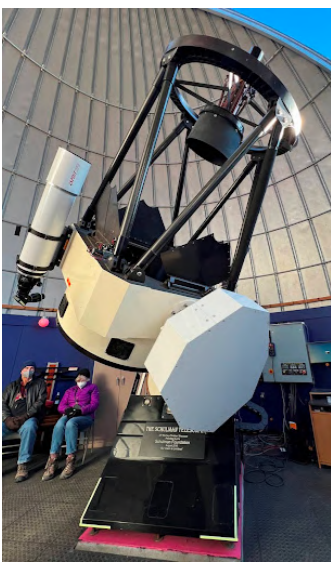
<http://project-eden.space/team>

- We observed with seven telescopes across the Northern Hemisphere: four located in Arizona, two in Europe, and one in Taiwan.
- Under ideal scheduling and weather conditions, this longitudinal coverage allows for continuous observations of target stars visible from all sites.
- The telescope apertures range in size from 0.8 to 2.3 m.

EDEN Sites and Telescopes



Telescope	Location	Mount	CCD Imager
Phillips 0.6 m	Mount Lemmon, Arizona	EQ	SBIG STX (KAF-16803)
Schulman 0.8 m	Mount Lemmon, Arizona	EQ	SBIG STX (KAF-16803)
Lulin 1.0 m	Mount Lulin, Taiwan	EQ	Sophia 2048B CCD
Calar Alto 1.23 m	Calar Alto, Spain	EQ	DLR-MKIII camera with e2v CCD231-84-NIMO-BI-DD sensor
Cassini 1.52 m	Mount Orzale, Italy	EQ	Bologna Faint Object Spectrograph and Camera
Kuiper 1.55 m	Mount Bigelow, Arizona	EQ	Mont4K SN3088 (Weiner et al. 2018)
VATT 1.8 m	Mount Graham, Arizona	Alt-Az	VATT4K STA0500A CCD
Bok 2.3 m	Kitt Peak, Arizona	EQ	90 Prime Focus Wide-Field Imager (Grant Williams et al. 2004)



**Schulman
0.8 m**

**Lulin
1.0 m**

**Calar Alto
1.23 m**

**Cassini
1.52 m**

**Kuiper
1.55 m**

**VATT
1.8 m**

**Bok
2.3 m**

Telescope	Location	Det. Size	FOV	Operation
Phillips 0.6 m	Mount Lemmon, Arizona	4096 × 4096	22' × 22'	Robotic
Schulman 0.8 m	Mount Lemmon, Arizona	4096 × 4096	22' × 22'	Robotic
Lulin 1.0 m	Mount Lulin, Taiwan	2048 × 2048	13'08 × 13'08	Classical
Calar Alto 1.23 m	Calar Alto, Spain	4k×4k	21'5 × 21'5	Remote
Cassini 1.52 m	Mount Orzale, Italy	1300 × 1340	13' × 12'6	Classical
Kuiper 1.55 m	Mount Bigelow, Arizona	4096 × 4097	9'7 × 9'7	Classical
VATT 1.8 m	Mount Graham, Arizona	4064 × 4064	12'5 × 12'5	Classical
Bok 2.3 m	Kitt Peak, Arizona	4 × 4032 × 4096	1°16 × 1°16	Classical

- The Schulman 0.8 m telescope is robotically operated, while the CAHA 1.2 m is remotely operated.
- The rest require an on-site operator/observer each night.

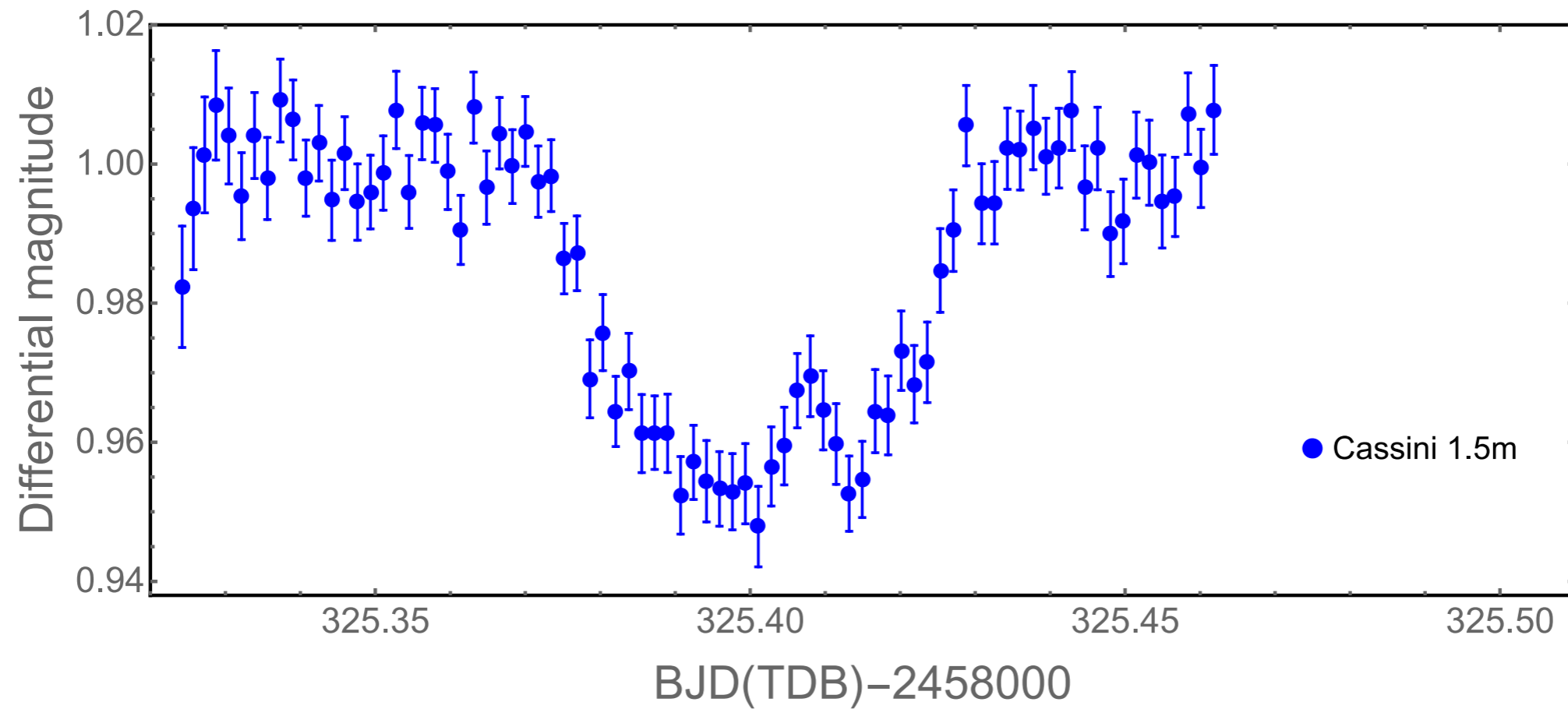
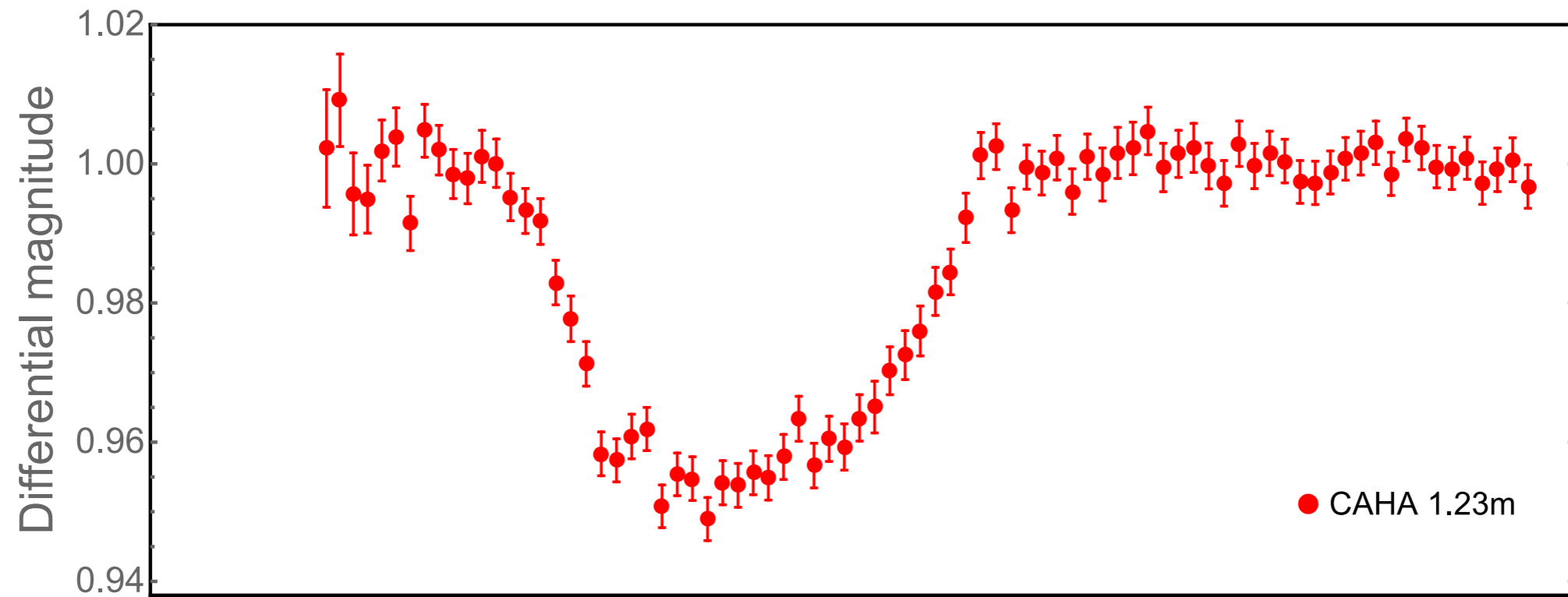
CA 1.23 m



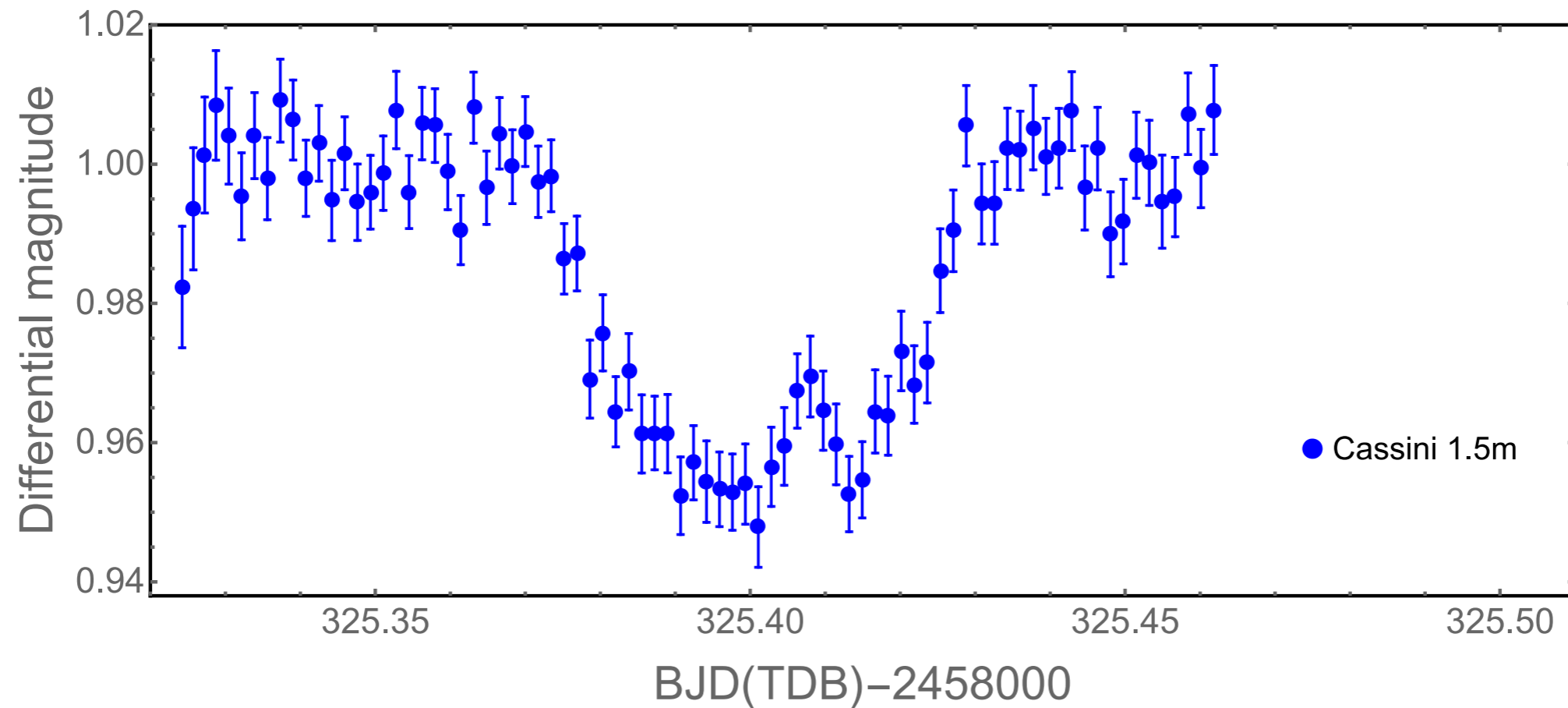
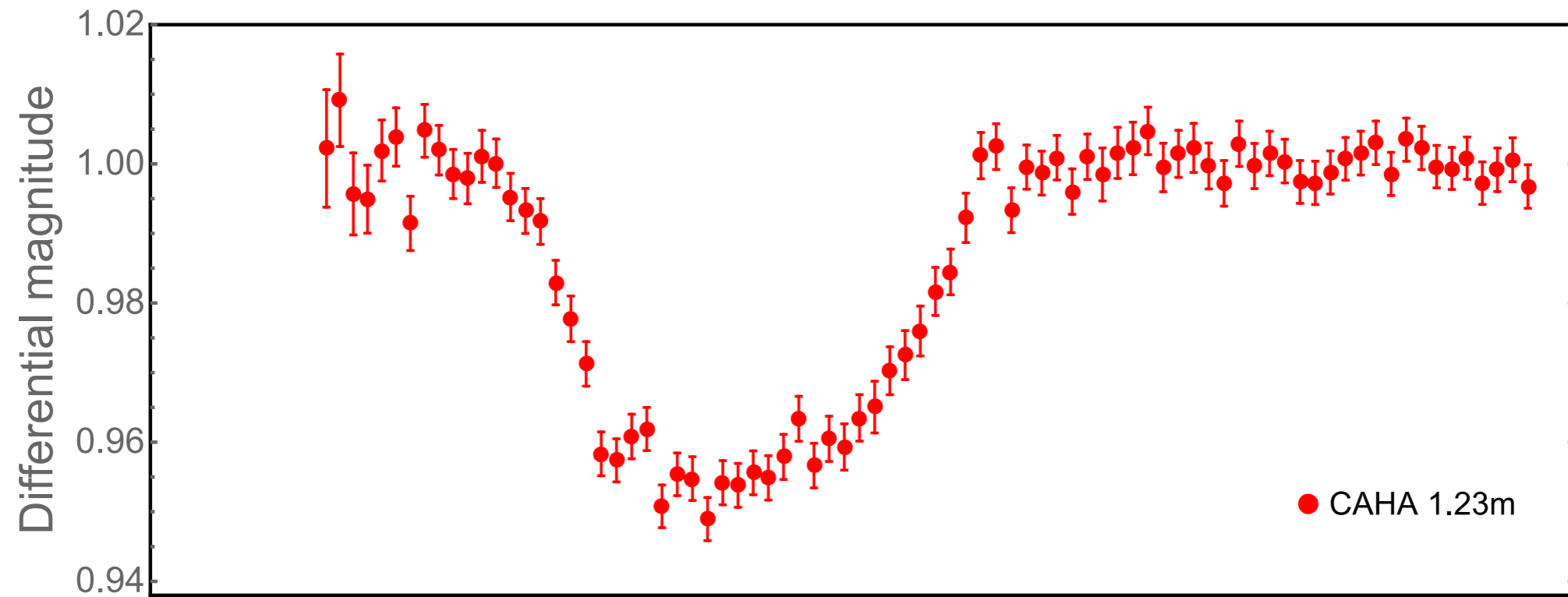
Cassini 1.52 m



WTS-2b ($V=15.9$ mag)



WTS-2b ($V=15.9$ mag)

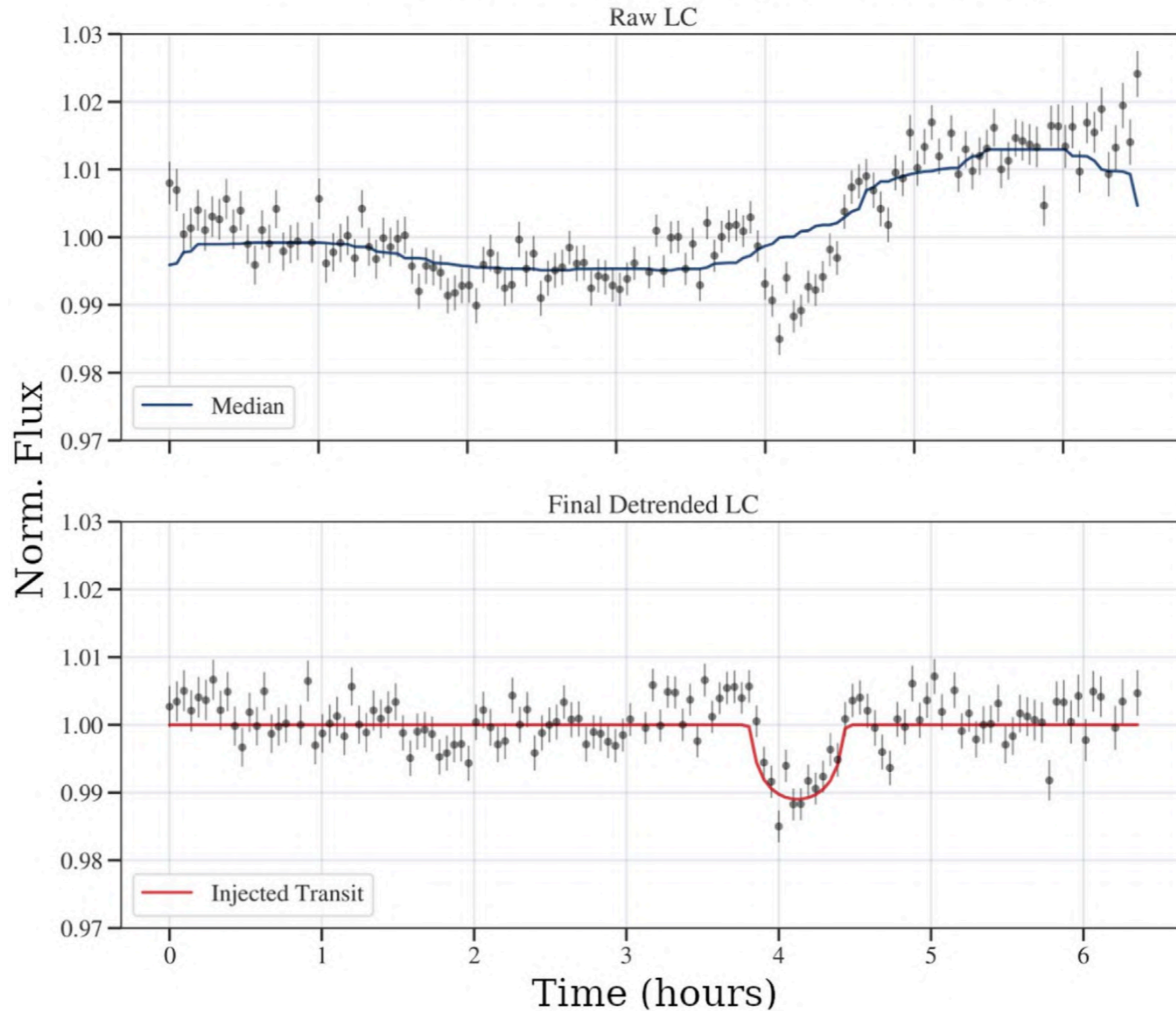


- The Project EDEN target list is comprised of all known single non variable stars of spectral type M7–L0 within 15 pc and with declinations $> -20^\circ$.

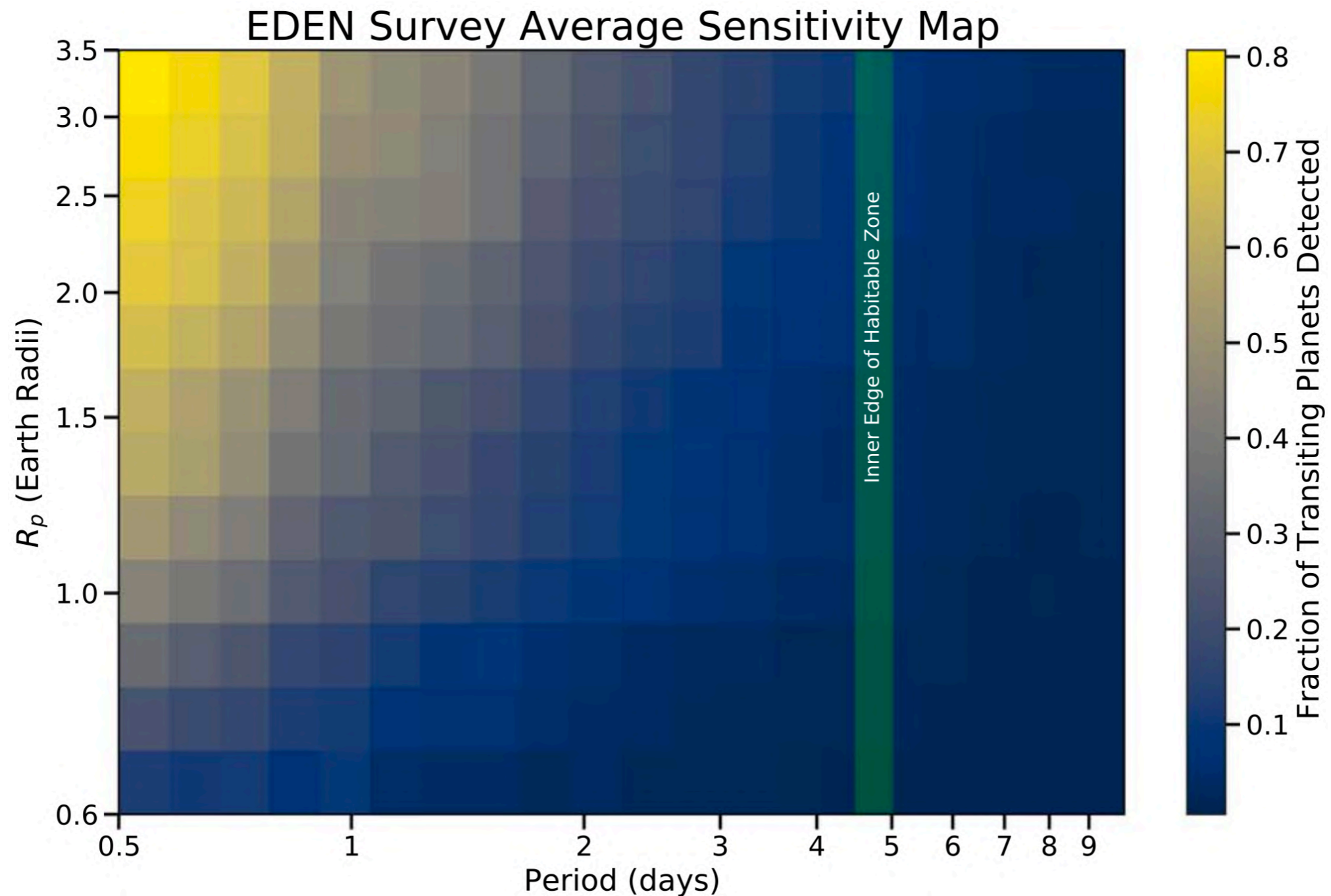
EIC ID	Gaia DR3 ID	R.A. (J2000) h:m:s	Decl. (J2000) d:m:s	PM R.A. mas/yr	PM Decl. mas/yr	Distance pc	Spectral Type	G (mag)	hr Obs.
1	2091177593123254016	18:35:37.88	32:59:53.3	-72.65 ± 0.05	-755.15 ± 0.05	5.689 ± 0.002	M8.5V	14.8510	204.0
2	56252256123908096	3:20:59.71	18:54:22.8	352.29 ± 0.09	-257.07 ± 0.08	14.648 ± 0.017	M8V	16.1048	324.8
4	2531195858721613056	1:09:51.20	-3:43:26.4	372.17 ± 0.27	8.65 ± 0.16	10.568 ± 0.023	M9Ve	16.3750	176.2
5	31235033696866688	3:14:03.44	16:03:05.5	-242.96 ± 0.19	-54.85 ± 0.16	13.768 ± 0.036	L0	17.2427	100.0
6	445100418805396608	3:30:48.89	54:13:55.2	-151.99 ± 0.04	3.42 ± 0.04	10.502 ± 0.004	M7V	13.7143	47.9
7	3257243312560240000	3:51:00.03	-0:52:44.9	10.99 ± 0.06	-469.97 ± 0.05	14.678 ± 0.015	M8.0V	15.3131	47.5
8	230171768457140736	3:57:19.98	41:07:42.6	-204.37 ± 0.06	-24.74 ± 0.05	14.183 ± 0.012	M7V	14.6381	106.4
9	229155579195699456	4:19:52.13	42:33:30.4	528.67 ± 0.08	-1441.61 ± 0.06	10.262 ± 0.010	M8.5V	15.5551	411.3
11	3200303384927512960	4:40:23.27	-5:30:08.1	334.53 ± 0.06	127.91 ± 0.06	9.747 ± 0.006	M7	14.9043	49.1
12	3421840993510952192	5:10:20.09	27:14:01.9	-213.27 ± 0.08	-630.81 ± 0.06	10.276 ± 0.007	M7V	14.9257	213.0
13	191109281417914880	5:39:24.80	40:38:42.8	646.15 ± 0.09	-834.49 ± 0.05	11.367 ± 0.010	M8.0	15.2733	49.4
14	1097353325107339776	8:25:52.82	69:02:01.1	-691.17 ± 0.29	-1276.32 ± 0.39	12.289 ± 0.059	M7V	13.7621	57.0
15	5761985432616501376	8:53:36.16	-3:29:32.2	-516.61 ± 0.08	-199.65 ± 0.05	8.659 ± 0.005	M9.0	15.8889	65.1
16	1227705135863076864	14:28:04.16	13:56:13.3	-365.42 ± 0.06	-495.51 ± 0.06	13.230 ± 0.010	M7V	14.8963	57.3
17	1287312100751643776	14:28:43.23	33:10:39.3	-346.96 ± 0.04	-710.99 ± 0.09	10.969 ± 0.012	L0	16.6346	219.8
18	1282632682337912832	14:44:17.18	30:02:14.2	-94.39 ± 0.07	-340.33 ± 0.07	14.781 ± 0.015	M8e	15.9061	80.2
19	1262763648230973440	15:01:08.19	22:50:02.1	-43.12 ± 0.11	-65.14 ± 0.14	10.734 ± 0.016	L0	16.5353	64.5
20	1272178319624018816	15:24:24.76	29:25:31.5	-56.77 ± 0.03	-629.24 ± 0.04	13.078 ± 0.008	M7.5V	15.2801	95.7
21	6265453524968112640	15:34:56.93	-14:18:49.3	-918.81 ± 0.14	-330.23 ± 0.10	10.938 ± 0.013	M8.6V	15.7637	45.4
22	4588438567346043776	18:26:11.00	30:14:18.9	-2290.75 ± 0.09	-683.27 ± 0.09	11.101 ± 0.010	M8.5V	15.9470	80.2
23	1762523981210977664	20:44:37.48	15:17:34.8	303.68 ± 0.06	-155.49 ± 0.05	10.395 ± 0.006	M8	15.2678	27.4

- Data reduction was performed with a custom Python-based automatic pipeline.
- To search for transits in our light curves, we utilized the package Transit Least Squares (TLS; Hippke & Heller 2019).
- We optimized the TLS algorithm for our search by setting upper and lower limits on the stellar radius and mass to those for M dwarfs ($0.1 - 0.6 R_{\odot}$, $0.08 - 0.5 M_{\odot}$) and the maximum period to correspond to the approximate outer edge of the habitable zone (~ 10 days).
- To estimate our sensitivity for transit signals, we employed injection-and-retrieval simulations.
- Our approach was to inject planet signatures on a grid of orbital period versus planet radius and recover them.

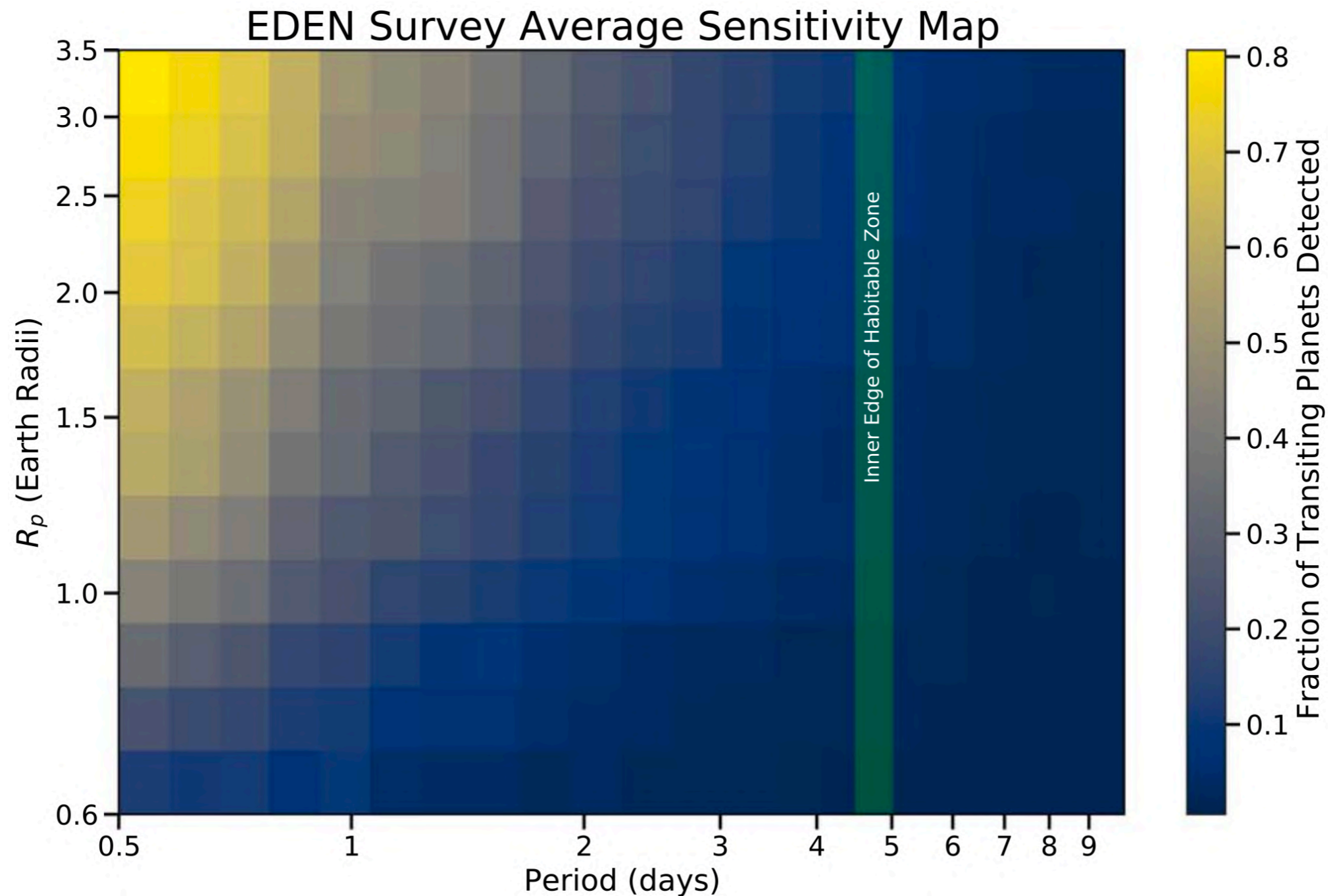
EIC-2 (LP 412-31) Example Detrending



- Data were taken with the Cassini telescope on 2018 December 11. The red line at the bottom shows the injected transit signal (depth $\sim 1\%$, TRAPPIST-1b orbit) compared to the light curve after median detrending has been applied (Gibbs et al. 2020, AJ 159, 169).

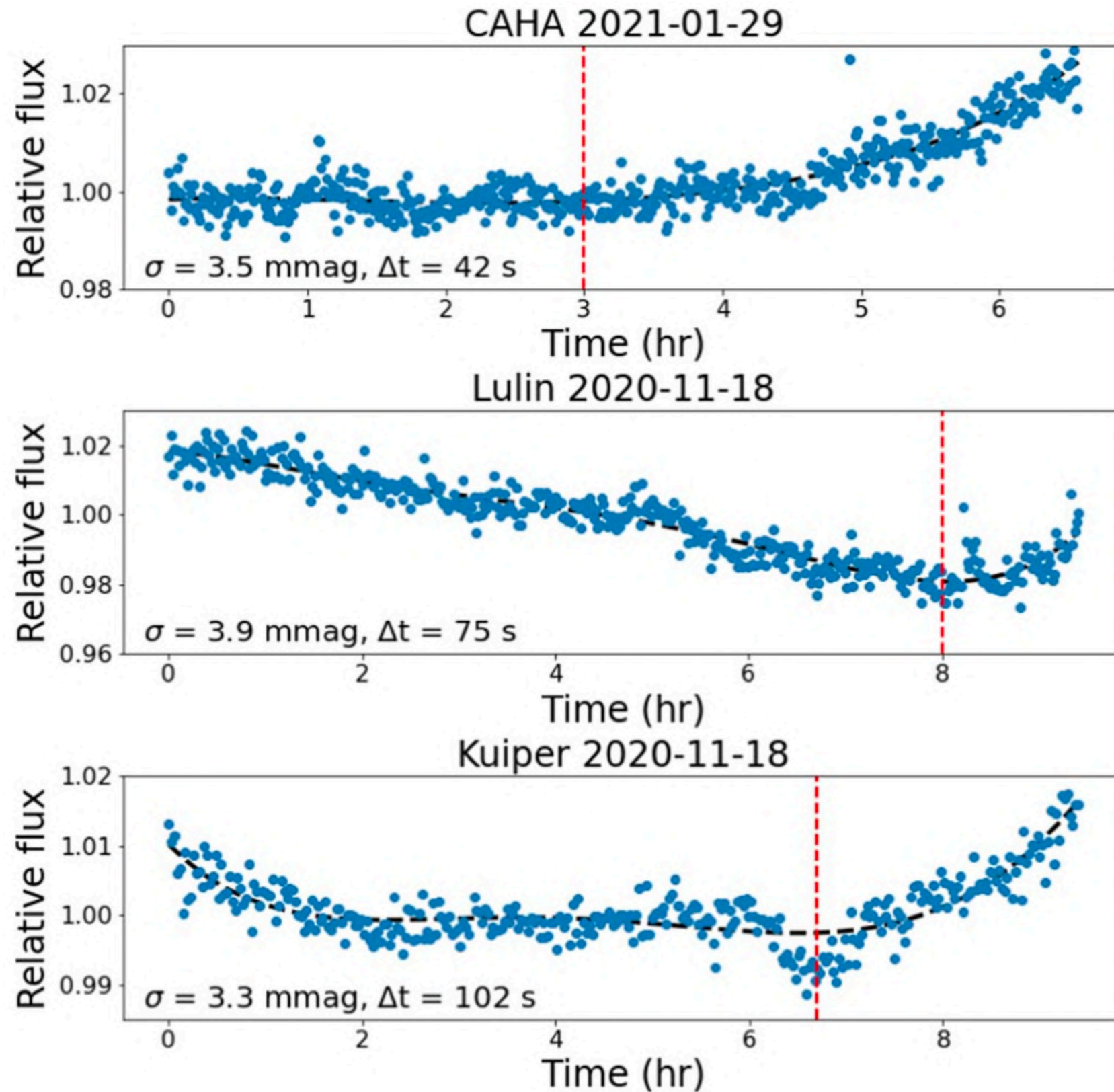


- We use transit injection-and-recovery tests to quantify the completeness of our survey,
 - successfully identify most ($> 80\%$) transiting short-period (0.5 – 1 days) super-Earths ($R_p > 1.9 R_{\oplus}$),
 - and being sensitive ($\sim 50\%$) to transiting short-period Earth-sized planets ($R_p = 1.0 - 1.2 R_{\oplus}$).

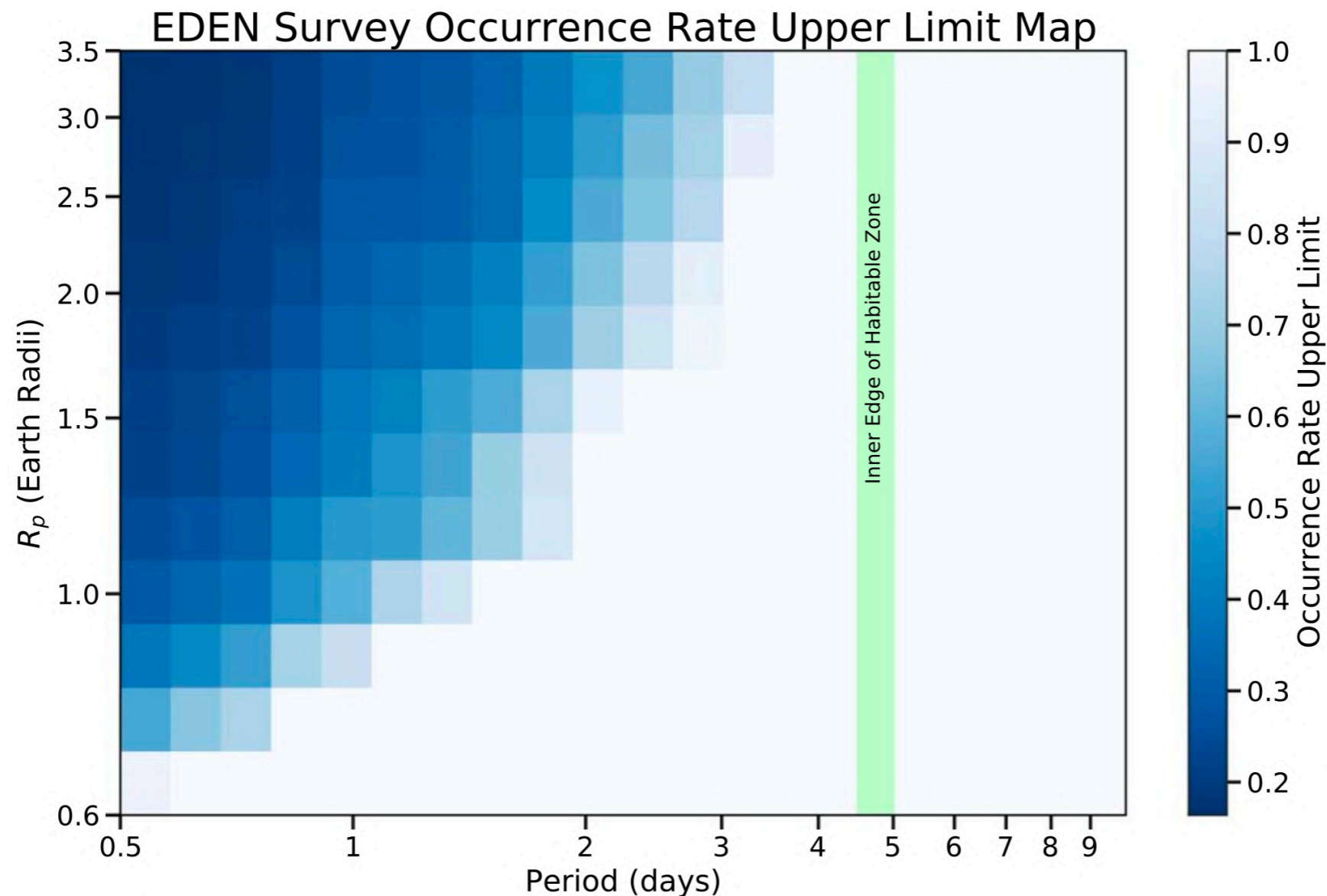


- Our average sensitivity to Neptune-sized planets ($R \sim 3.5 R_{\oplus}$) on very short ($P \sim 0.5$ days) orbits for most of our target stars is $\sim 85\% - 90\%$.
- This can be extended as a conservative estimate to larger planets as well.
- Our average sensitivity to TRAPPIST-1b-like planets is $\sim 30\%$.

- Our survey does not yield a transiting planet detection.



- Following the approach by Seager et al. (2020), we set the probability of seeing zero planets around 22 ultra-cool dwarfs to less than 5%, and we calculated the upper limit of true planet occurrence η for several binned planet type.
- In bins where our survey has low efficiency, we have no information on the true occurrence rate, so the upper limit on η is 1.0.



- We also simulated observations of synthetic planets in the measured EDEN light curves, with the planet parameters drawn from model distributions corresponding to the specific hypothesis tested.
 - For example, a TRAPPIST-1b-like planet would be a $1.1 R_{\oplus}$ planet orbiting at $P = 1.5$ days with a random orbital inclination.
- We then determined in what fraction of the simulated surveys the number of detections would be consistent (at 2σ) with the outcome of the EDEN survey.
 - For example, if our survey resulted in zero planet detections, but our hypothesis would lead to planet detections in 95% of the simulated surveys, we would be able to exclude that hypothesis at the 95% confidence level.

- We tested the hypothesis that “TRAPPIST-1 b analogs orbit every late-M dwarf star”.
- We simulated our EDEN transit survey 10,000 times to determine in what fraction of these surveys would the predicted results be consistent with our actual survey.
- Assuming isotropic orbit orientations, we injected a planet with probability $P_{\text{geom}} = (R_{\star} + R_{\text{p}})/a$, which approximates the geometric transit probability for a planet with radius R_{p} in a circular orbit with semi-major axis a around a star with radius R_{\star} .
- In the case of a transit occurring, we injected the photometric signature of a planet with a random orbital phase and TRAPPIST-1b’s orbital period and planet radius ($P = 1.511$ days, $R_{\text{p}} = 1.16 R_{\oplus}$, respectively) and tested its detection by our pipeline.
- In 15% of our simulated surveys, we would have seen at least one planet out of our sample of 22 stars.

- Finally we tested the fraction of late-M dwarfs hosting a giant planet at a short orbital period $P = 1.05$ days.
- For a host-star radius representative of an M8V dwarf ($R_{\star} = 0.114 R_{\odot}$) the geometric transit probability $P \approx 11\%$ for a planet in a 1.05 day orbit.
- Even assuming such close orbits, 98% of our mock surveys yield zero detections if giant planets occur around 2% of late- M dwarfs (Ghezzi et al. 2018).
- If instead every such star hosts a giant planet, we would expect to detect at least one giant planet in our survey in 73% of the cases.
- If we decrease the orbital period down to 0.5 day orbital periods, the average sensitivity to a transiting planet increases by a factor of ~ 1.6 , and we can constrain the giant planet occurrence rate down to 75% with 95% confidence.

Conclusions

- The current detection numbers of small planets orbiting M stars is low (<10).
- Improved occurrence rate estimates are an important feedback for planet formation theories, which can be constrained by comparing synthesized planet populations to observed samples.
- The EDEN survey yielded a rich data set of detrended light curves with $\sim 1 - 10$ mmag scatter for 22 target stars ranging in spectral types from M7V to L0, and in distance from 5.7 to 14.8 pc.
- For most target stars, our data set provides the highest- quality photometric monitoring to date, often with a unique combination of relatively high cadence (~ 60 s), sensitivity, and monitoring baseline.
- The light curves were used in this study to search for transiting exoplanets and place upper limits on their occurrence rates, but they can also be exploited for studies of stellar activity and stellar rotation, among other uses.
- Our survey did not yield any transiting-planet detections, however, blind, volume-limited surveys still provide the least biased studies of mid- to late-M dwarfs.

Conclusions

- We tested the fraction $f_{\text{Tr,b}}$ of late-M dwarfs hosting a TRAPPIST-1 b analog planet and f_{Tr} of a TRAPPIST-1 analog system.
- Given no detections in our survey, and the well-characterized sensitivity, we cannot exclude $f_{\text{Tr,b}} < 100\%$ (15% of surveys would detect a planet) nor an $f_{\text{Tr}} < 100\%$ (21% of surveys would detect a planet).
- Additionally, we tested the fraction f_{large} of late-M dwarfs hosting a giant planet at a short orbital period $P = 1.05$ days. We found that we cannot exclude $f_{\text{large}} < 100\%$ with 73% of the simulated surveys detecting a planet.
- However, at 0.5 day orbital periods, we can constrain $f_{\text{large}} < 75\%$ at a 95% confidence level.

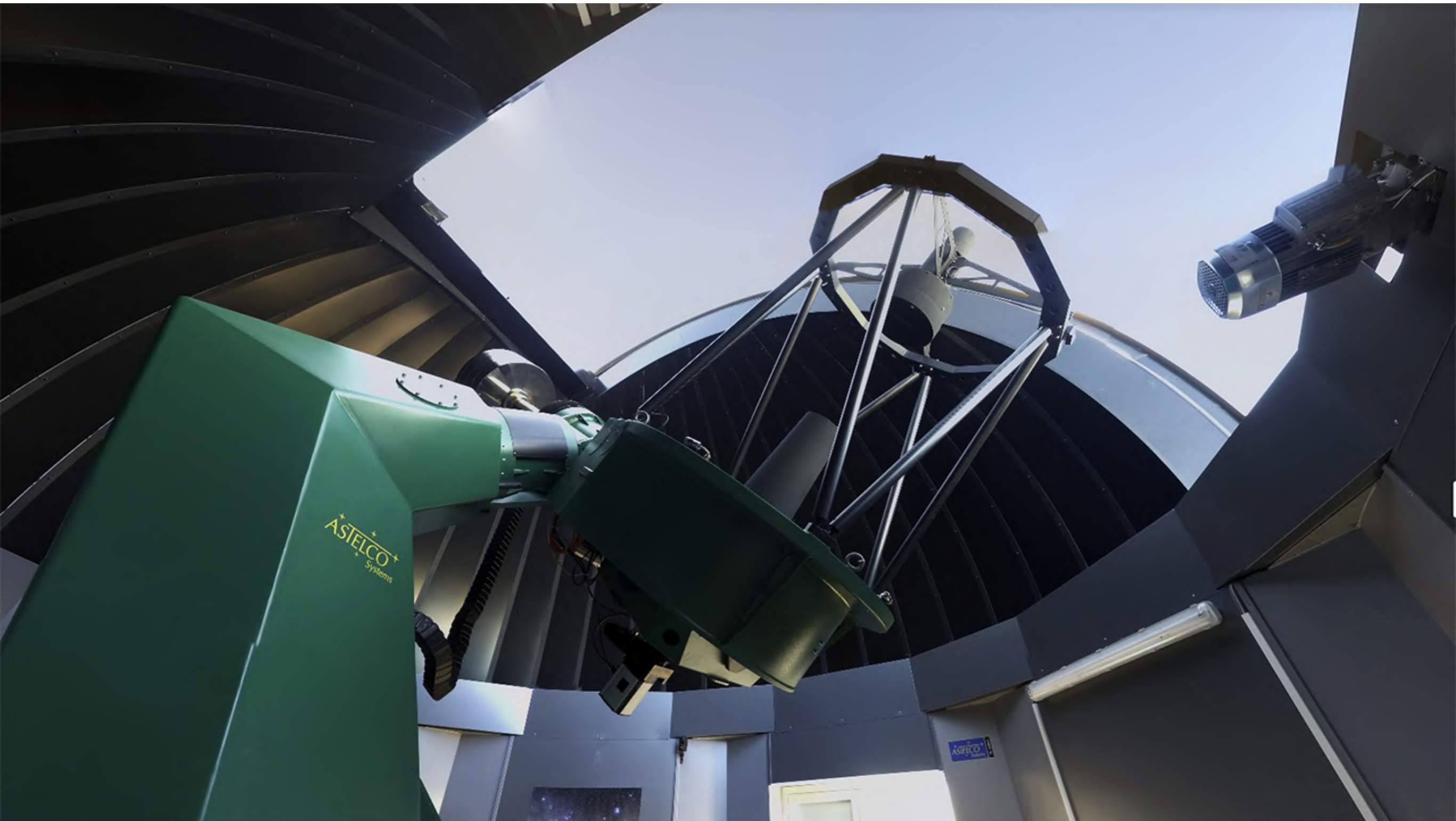
THANK YOU

- Data reduction was performed with a custom Python-based automatic pipeline.
- The first step was to calibrate the raw science frames using the standard calibration frames (bias, flat).
- Astrometric solution was derived for every science frame.
- After the calibration, aperture photometry was performed.
- For every star in the field of view, we measured the intensity in apertures ranging from 5 to 50 pixels in steps of 1 pixel.
- The aperture size that minimized the rms scatter of the target-star light curve was selected as the best aperture for all sources.
- Sky background was calculated as the median of a 60×60 pixel sub-image around the star with other sources clipped.
- Photometry was saved into a file with other important information for each star, such as centroid positions, stellar magnitudes, background, FWHM, airmass, etc., useful for detrending steps and vetting transit-like signals.

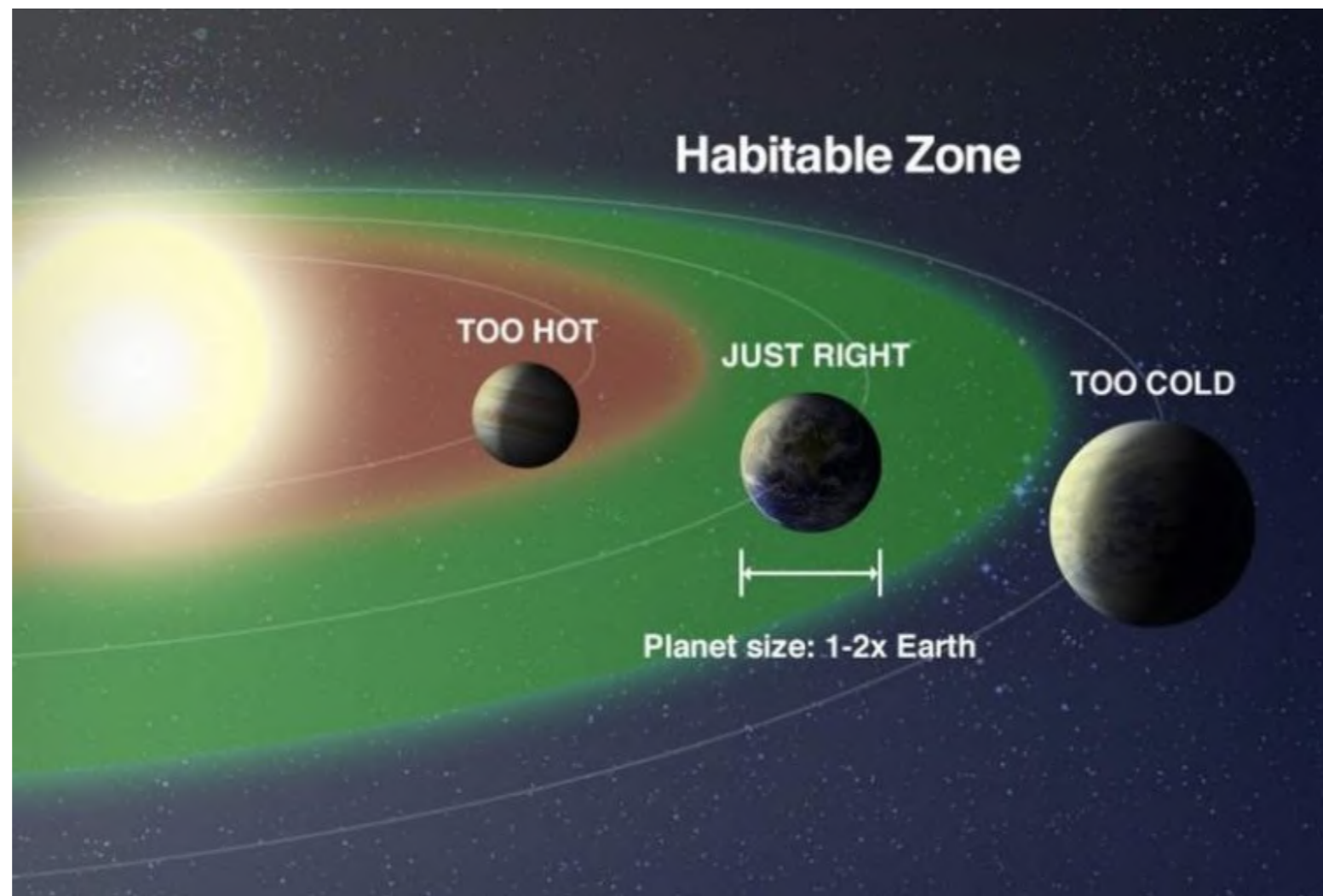
- The next step was to detrend the target light curve on the basis of comparison star light curves.
- Trends are long- or short-term photometric variations in the light curve that decrease transit detection sensitivity, and can arise from instrumental, atmospheric, and stellar variability.
- We selected the best comparison stars by first filtering out stars that are saturated, are too faint (several magnitudes dimmer than the target), or have too many failed photometric measurements.
- Next, we divided the flux-normalized target light curve by the normalized light curves of every comparison star, and rank them based on the average standard deviation in windows of 20 data points.
- The six with the lowest average deviation (i.e., those with the most similar data trends) are median-combined into a “super comparison” light curve, which the target light curve is then divided by.

- To final step was to search for transits in our detrended light curves.
- For this purpose, we utilized the package Transit Least Squares (TLS; Hippke & Heller 2019).
- We optimized the TLS algorithm for our search by setting upper and lower limits on the stellar radius and mass to those for M dwarfs ($0.1 - 0.6 R_{\odot}$, $0.08 - 0.5 M_{\odot}$) and the maximum period to correspond to the approximate outer edge of the habitable zone (~ 10 days).
- Besides the geometric probability of a planet to transit given our line of sight to its host star, the completeness of our survey is limited by our ability to detect transit signatures.
- Our sensitivity is mostly limited by the photometric precision of our light curves and by the performance of our detection pipeline.
- To estimate our sensitivity for transit signals, we employed injection-and-retrieval simulations.
- Our approach was to inject planet signatures on a grid of orbital period versus planet radius and recover them.

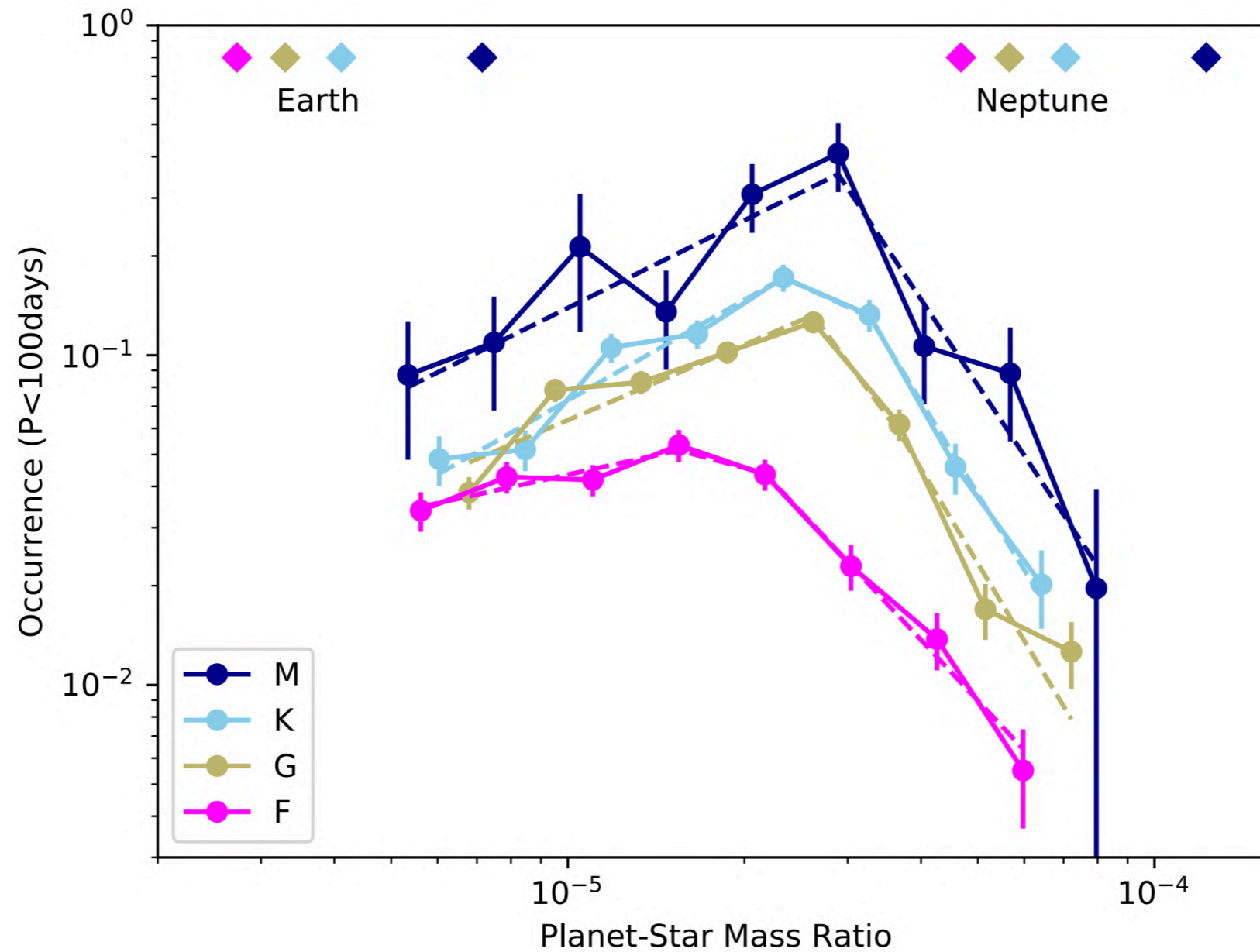
- SPECULOOS-North is the Northern counterpart of SPECULOOS-South. It is located at Teide Observatory in the island of Tenerife (Canaries).



- Additionally, their habitable zone lies much closer to the host star, thus improving their geometric transit probability: for an M5V star, a planet receiving the same stellar flux as the Earth would lie only 0.074 au from the star, presenting a 1.6% geometric transit probability, $3.2\times$ greater than the value for the G2V planet.
- Such planets may spend billions of years in the habitable zone.



- Short-period rocky planet occurrence rates were found to be about 3.5 greater around M-dwarfs than around sun-like stars (Dressing & Charbonneau 2015, ApJ 807, 45, 2015; Mulders et al., ApJ 798, 112, 2015).



Pascucci et al., ApJ 856, 28 (2018)